PHILOSOPHICAL TRANSACTIONS OF THE ROYAL SOCIETY A MATHEMATICAL, PHYSICAL & ENGINEERING SCIENCES

The Formation of Magnetic Singularities by Time-Dependent Collapse of an X-Type Magnetic Field

E. R. Priest, V. S. Titov and G. Rickard

Phil. Trans. R. Soc. Lond. A 1995 **351**, 1-37
doi: 10.1098/rsta.1995.0024

The formation of magnetic singularities by time-dependent collapse of an X-type magnetic field

By E. R. Priest, V. S. Titov† and G. Rickard

Mathematical and Computational Sciences Department, The University, St Andrews, KY16 9SS, U.K.

Contents

A self-consistent solution is presented for nonlinear time-dependent collapse of a two-dimensional X-type magnetic field to form a current sheet. A so-called 'strong magnetic field approximation' is adopted for highly sub-Alfvenic flow of an ideal low-beta plasma. To lowest order in the Alfven Mach number, the magnetic field evolves through a series of topologically accessible piece-wise potential states with the constraint that the acceleration be perpendicular to the magnetic field. A wide class of solutions is obtained using complex variable theory by assuming the magnetic potential is frozen to the plasma. The current sheet in the basic solution stretches along the x-axis from $-\sqrt{t}$ to $+\sqrt{t}$, and regions of reversed current are found near the ends of the sheet. A current conservation theorem is proved, which states that the total current in the sheet is zero if it forms

† Permanent address: Program Systems Institute, Academy of Sciences, Pereslavl-Zalessky 152140, Russia.

Phil. Trans. R. Soc. Lond. A (1995) **351**, 1–37
Printed in Great Britain

by collapse of an initially current-free X-point under the strong magnetic field approximation and with the magnetic potential frozen to the plasma. The basic solution is generalized to include other initial states and initial flows. A general numerical method for the evolution of magnetic fields under the strong magnetic field approximation is set up when the magnetic potential is not necessarily frozen to the plasma. This method is applied to an example of the formation of a current sheet with Y-type neutral points at its ends.

1. Introduction

X-points are special points in a complex two-dimensional magnetic field where the magnetic field vanishes, and near which the field structure is hyperbolic in nature. The magnetic field lines which pass through them are known as separatrices and they divide the magnetic field up into topologically separate regions. The X-points represent weak spots in the structure in the sense that the motions of distant sources can make the field near such a point collapse to form a current sheet, where the magnetic field is no longer frozen to the plasma. As a result, rapid dissipation of the magnetic field occurs, with the magnetic energy being converted into heat, kinetic energy and fast-particle energy by the process of magnetic reconnection (see, for example, Priest 1985). In most of the solar atmosphere, the magnetic field is frozen to the plasma and magnetic energy cannot be converted directly into heat, but such current sheets are a prime candidate for energy conversion in many solar phenomena, such as solar flares (Priest 1981; Somov 1992; Svestka *et al.* 1992), X-ray bright points (Priest *et al.* 1994) and the heating of coronal loops (Parker 1972; Ulmschneider *et al.* 1991; Priest 1993). In three dimensions, the X-point becomes a separator field line (which may join three-dimensional null points) while the separatrix field lines become separatrix surfaces, but locally, in a plane perpendicular to a separator, the behaviour is likely to be predominantly similar to the two-dimensional behaviour described here.

However, it is not only in the solar atmosphere that X-points are important. Most of the universe is in the plasma state and magnetohydrodynamics (MHD) is relevant when the length-scales of interest exceed the appropriate plasma scales (the mean-free path or ion gyro-radius). According to the basic MHD equations, for most reasonable length-scales of interest, the magnetic field is frozen to the plasma and is carried around with it. It is only in current sheets (which tend to form from X-points) that the magnetic field diffuses through the plasma and the magnetic energy can be released. Thus, current-sheet formation at X-points is thought to be important in a wide range of astrophysical and space plasma phenomena, some of which are analogies of solar phenomena (such as stellar flares, stellar coronal heating and geomagnetic substorms), while others have no solar analogy (such as the creation of magnetic turbulence in accretion discs). In addition, the formation of current-sheet singularities in magnetic fields has analogous formation of vortex sheets in Euler flows in ordinary fluid dynamics (Moffatt 1985, 1990; Linardatos, 1993).

Thus, the manner in which X-points collapse to form current sheets is a key problem in MHD. Dungey (1953) was the first to argue on physical grounds that

PHILOSOPHICAL TRANSACTIONS OF THE ROYAL SOCIETY A MATHEMATICAL, PHYSICAL & ENGINEERING SCIENCES

X-points may be locally unstable to collapse. Consider, for example, the simple equilibrium current-free field

$$B_x = \frac{B_0 y}{\ell}, \quad B_y = \frac{B_0 x}{\ell} \tag{1.1}$$

near an X-type neutral point at the origin, where B_0 and ℓ are constants. The field lines are the rectangular hyperbolae

$$y^2 - x^2 = \text{const.} \tag{1.2}$$

Now suppose the field is distorted to the form

$$B_x = \frac{B_0 y}{\ell}, \quad B_y = \alpha^2 \frac{B_0 x}{\ell}, \tag{1.3}$$

where $\alpha^2 > 1$. The corresponding field lines are given by

$$y^2 - \alpha^2 x^2 = \text{const.}, \tag{1.4}$$

so that the limiting separatrix field lines ($y = \pm\alpha x$) through the origin are no longer inclined at $\frac{1}{2}\pi$ but have closed up a little like a pair of scissors.

The current density ($\boldsymbol{j} = \nabla \times \boldsymbol{B}/\mu$) that results from field (1.3) has only a z-component $j_z = (\alpha^2 - 1)B_0/(\mu\ell)$. It is uniform in space and gives a Lorentz force

$$\boldsymbol{j} \times \boldsymbol{B} = -\frac{(\alpha^2 - 1)\alpha^2 x B_0^2}{\mu\ell}\hat{\boldsymbol{x}} + \frac{(\alpha^2 - 1) y B_0^2}{\mu\ell}\hat{\boldsymbol{y}}. \tag{1.5}$$

On the x-axis, the field lines are more closely spaced but with a smaller curvature than initially and so the inwards magnetic pressure force increases while the tension force decreases, giving a resultant magnetic force towards the origin. On the y-axis, the field lines have the same spacing as initially, but are more sharply curved, so that the pressure force remains the same and the tension force increases, producing an outwards magnetic force. In other words, the magnetic force is such as to increase the original perturbation. As the instability proceeds, α increases and the separatrices close up, so that the current density and ohmic heating $j^2\eta\mu$ also increase.

The instability may be demonstrated formally by showing that the linearized form of the ideal (MHD) low-β equations, namely

$$\frac{\partial \boldsymbol{B}}{\partial t} = \nabla \times (\boldsymbol{v} \times \boldsymbol{B}), \quad \rho \frac{\mathrm{d}\boldsymbol{v}}{\mathrm{d}t} = (\nabla \times \boldsymbol{B}) \times \boldsymbol{B}/\mu, \quad \frac{\mathrm{d}\rho}{\mathrm{d}t} = -\rho \nabla \cdot \boldsymbol{v}, \tag{1.6}$$

possess solutions of the form

$$\left.\begin{aligned} B_x &= B_0[1 - \epsilon \mathrm{e}^{\omega t}]y/\ell, & B_y &= B_0[1 + \epsilon \mathrm{e}^{\omega t}]x/\ell, \\ v_x &= -\epsilon v_\mathrm{A} \mathrm{e}^{\omega t} x/\ell, & v_y &= \epsilon v_\mathrm{A} \mathrm{e}^{\omega t} y/\ell, \end{aligned}\right\} \tag{1.7}$$

where B_0, $\rho = \rho_0$, $v_\mathrm{A} = B_0/(\mu\rho_0)^{1/2}$, ϵ ($\ll 1$) are constants and the growth-rate is

$$\omega = 2v_\mathrm{A}/\ell. \tag{1.8}$$

The two-dimensional collapse of an X-type configuration was later investigated more fully by others. Imshennik & Syrovatsky (1967) discovered a nonlinear self-similar compressible solution with a uniform density, which indicates that the

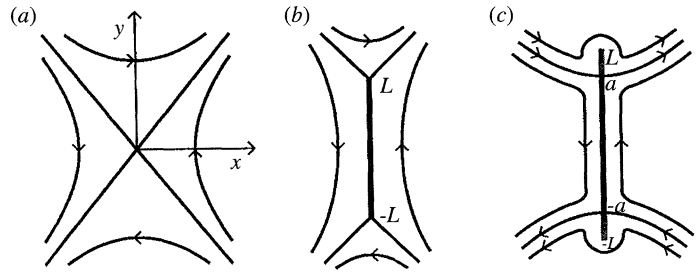

Figure 1. (a) A potential magnetic field near an X-type neutral point; (b) a current sheet with null points at its ends; and (c) a current sheet with reversed current regions near its ends.

collapse takes a multiple of the Alfven time ℓ/v_{A}. Forbes & Speiser (1979) and Forbes (1982) modelled the one-dimensional implosion of a magnetic field to form a current sheet. Syrovatsky (1966, 1969, 1971) studied the response to a small motion of the sources and included the idea in a solar-flare model. More recently, Craig & McClymont (1991) have included magnetic diffusion in a linear analysis of a small perturbation of an X-type field.

Another strand of the theory was initiated by Green (1965), who modelled the appearance of a current sheet near the X-point, by using complex-variable theory, and treated the current sheet as a cut in the complex plane. He considered the slow deformation of a two-dimensional potential field containing an X-point in the perfectly conducting limit and supposed that the X-point bifurcates into a pair of Y-type neutral points joined by a current sheet (figure 1).

By absorbing the constants B_0 and ℓ in the magnetic field and the spatial coordinates, the field (1.1) may be written compactly in terms of the complex variable $z = x + \mathrm{i}y$ as

$$B_y + \mathrm{i}B_x = z. \tag{1.9}$$

The current-sheet field which may grow from this is given by

$$B_y + \mathrm{i}B_x = (z^2 + L^2)^{1/2}, \tag{1.10}$$

where the sheet stretches from $z = -\mathrm{i}L$ to $z = +\mathrm{i}L$.

It should be noted that solutions such as (1.10) may be used in three distinct ways. First, it represents an equilibrium field which is potential everywhere except at the current sheet separating two topologically different magnetic flux systems. Second, by allowing L to vary slowly in time and not allowing reconnection in the sheet, it may model the time-dependent growth of a current sheet from the X-point and the resulting evolution of the surrounding potential field. Third, by allowing reconnection in the sheet, it may model the process of nonlinear magnetic reconnection at a rate much slower than the Alfven speed (so that the surrounding field is potential) when the effect of slow-mode shock waves propagating from the ends of the current sheet is negligible (as is sometimes the case in recent numerical experiments at high magnetic Reynolds number (Biskamp 1986)). This approach has been developed by Priest & Lee (1990) and Strachan & Priest (1994) in their model of *non-uniform reconnection*. The complex flux function $f = A + \mathrm{i}\Phi$ corresponding to (1.10) is

$$f = -\tfrac{1}{2}z(z^2 + L^2)^{1/2} + \tfrac{1}{2}L^2 \log\left[z/L + \sqrt{(z^2/L^2 + 1)}\right] + F(t), \tag{1.11}$$

where $F(t)$ is a real function, determined in this model by resistive processes

PHILOSOPHICAL TRANSACTIONS OF THE ROYAL SOCIETY A MATHEMATICAL, PHYSICAL & ENGINEERING SCIENCES

within the sheet. (Including an imaginary part of F would give an arbitrary shift of magnetic potential Φ in time and would have no physical sense, so we can set it equal to zero without loss of generality.) The reconnection may be steady or non-steady by allowing L and $\mathrm{d}F/\mathrm{d}t$ to be constant or time-dependent. If F is a constant, there is no reconnection.

Green's approach has been extended and applied to several solar phenomena. Priest & Raadu (1975) modelled the formation of a current sheet in the corona between a pair of equal bipolar sunspot groups. Tur & Priest (1976) extended the analysis to include curved current sheets and applied it to unequal interacting bipoles and also to the sheet that is created as new flux emerges from below the photosphere into an overlying horizontal field (see also Low & Hu 1983). Tur (1977) generalized the Priest–Raadu analysis to the approach of three-dimensional dipoles creating an axisymmetric annular current sheet. Sakurai & Uchida (1977) have calculated curved current sheets between sets of dipoles. Also, Malherbe & Priest (1983) set up several current-sheet models for solar prominences, while Priest *et al.* (1989) have proposed a twisted flux-tube model for prominences in which the prominence is modelled as a current sheet in a large-scale twisted flux tube. Aly & Amari (1989) derived a general form for a magnetic field with current sheets. This enabled Titov (1992) to develop a general technique for calculating current-sheet fields from boundary conditions given at the photosphere.

Somov & Syrovatsky (1976) realized that the solution (1.10) is not unique and that there are other current-sheet solutions which may evolve from the X-point field (1.9). They have the form

$$B_y + \mathrm{i}B_x = \frac{z^2 + a^2}{(z^2 + L^2)^{1/2}}, \tag{1.12}$$

where $a^2 < L^2$, and have a sheet stretching from $z = -\mathrm{i}L$ to $\mathrm{i}L$ as before, but now there are singularities at the ends of the sheet and regions of reversed-current stretch from one null point at $z = \mathrm{i}a$ to $\mathrm{i}L$, and from another null point at $z = -\mathrm{i}a$ to $-\mathrm{i}L$. The particular case $a^2 = L^2$ reduces to (1.10). However, these solutions were largely ignored in the West until recent numerical experiments on magnetic reconnection sometimes revealed reversed-current spikes near the ends of the reconnecting current sheet (Biskamp 1986; Lee & Fu 1986; Forbes & Priest 1987). Also, Bajer (1990) has numerically modelled the collapse of an X-point in an isolated region and found that reversed and singular currents appear at the ends of the sheet.

A natural question that arises is: when an X-point collapses, is the resulting current sheet of the form (1.10) or (1.11), or is it of some other form? Furthermore, fields (1.10) and (1.11) are simply piecewise potential solutions of Laplace's equation that have cuts or current sheets, and have just been written down by inspection, so what solutions arise when one solves both the equation of motion (from which Laplace's equation arises) and the induction equation in a self-consistent manner? Here we attempt to shed light on these questions. We find some new self-consistent solutions to the MHD equations for the nonlinear ideal dynamic growth of a current sheet in the limit when the Alfven Mach number is much less than unity.

A preliminary analysis was presented by Titov & Priest (1993). Section 2 describes the equations and assumptions of the model. Section 3 gives the properties

of the solution and proves a theorem about the total current in the sheet. Section 4 generalizes the solution in several ways, and § 5 develops a technique for solving the problem numerically when the magnetic potential is not frozen to the plasma.

2. Equations and assumptions of the model

(a) *The strong magnetic field approximation*

Here we derive the basic equations for slow flow in an ideal cold plasma. First we assume that the plasma beta is much smaller and the magnetic Reynolds number much larger than unity, so that the plasma pressure gradient and the magnetic diffusion may be neglected and the equations of motion and induction may be written as

$$\rho \frac{\mathrm{d}\boldsymbol{v}}{\mathrm{d}t} = \boldsymbol{j} \times \boldsymbol{B}, \tag{2.1}$$

$$\frac{\partial \boldsymbol{B}}{\partial t} = \nabla \times (\boldsymbol{v} \times \boldsymbol{B}), \tag{2.2}$$

where

$$\boldsymbol{j} = \nabla \times \boldsymbol{B}/\mu, \quad \nabla \cdot \boldsymbol{B} = 0 \tag{2.3}$$

and the density ρ and pressure p are determined by the equations of continuity

$$\frac{\partial \rho}{\partial t} + \nabla \cdot (\rho \boldsymbol{v}) = 0 \tag{2.4}$$

and, say, adiabaticity

$$\frac{\mathrm{d}}{\mathrm{d}t}\left(\frac{p}{\rho^{\gamma}}\right) = 0. \tag{2.5}$$

Now suppose the flow is slow in the sense that flow speeds v are much smaller than the Alfven speed $v_{\mathrm{A}} = B/\sqrt{\mu\rho}$ and expand in powers of a small parameter $\varepsilon (\approx v/v_{\mathrm{A}})$:

$$\boldsymbol{v} = \varepsilon(\boldsymbol{v}_1 + \varepsilon \boldsymbol{v}_2 + \cdots), \quad \boldsymbol{B} = \boldsymbol{B}_0 + \varepsilon \boldsymbol{B}_1 + \cdots. \tag{2.6}$$

Assume also that time variations are on a time $\ell/v \sim \varepsilon^{-1}$, where ℓ is a typical length scale, and that the flow (v_x, v_y) and field (B_x, B_y) are two dimensional. Then, to lowest order, (2.1) and (2.2) become

$$\boldsymbol{j}_0 = \boldsymbol{0} \tag{2.7}$$

and

$$\frac{\partial \boldsymbol{B}_0}{\partial t} = \nabla \times (\boldsymbol{v}_1 \times \boldsymbol{B}_0). \tag{2.8}$$

In other words, there is an evolution through potential states ($\boldsymbol{j}_0 = 0$), with the plasma motion $v_{1\perp}$ perpendicular to the field lines determined by the frozen-in field-line motion. However, these potential states are not arbitrary, since they need to be 'accessible' with the topology being preserved (Moffatt 1985). Also, the flows need to be determined self-consistently. The above assumptions mean that any variations in time occur on the timescale of the fluid flow rather than the Alfven time. Thus, we are not considering magnetic waves and the question of the stability of our solutions is one for further study.

PHILOSOPHICAL TRANSACTIONS OF THE ROYAL SOCIETY A MATHEMATICAL, PHYSICAL & ENGINEERING SCIENCES

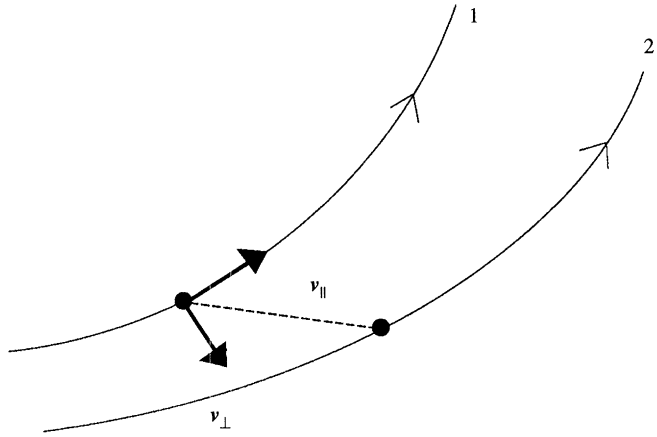

Figure 2. As a field line moves from position 1 to 2, the component $\boldsymbol{v}_\perp$ of the velocity of a plasma element is determined by the motion of the field line, while $\boldsymbol{v}_\parallel$ is determined by a balance between coriolis and centrifugal forces.

To next order, the equation of motion (2.1) gives

$$\rho_0 \frac{\mathrm{d}\boldsymbol{v}_1}{\mathrm{d}t} = \boldsymbol{j}_2 \times \boldsymbol{B}_0,$$

which implies a constraint at lowest order, namely that (Somov & Syrovatsky 1976)

$$\frac{\mathrm{d}\boldsymbol{v}_1}{\mathrm{d}t} \cdot \boldsymbol{B}_0 = 0. \tag{2.9}$$

In other words, the acceleration must be perpendicular to the magnetic field. This condition determines the flow $v_{1\parallel}$ parallel to the magnetic field from a balance between the coriolis and centrifugal forces associated with the rotation of the field lines as they move (figure 2).

The divergence-free condition (2.3) on the magnetic field may be satisfied identically by writing the field components in terms of the flux function A,

$$(B_{0x}, B_{0y}) = \left(\frac{\partial A}{\partial y}, -\frac{\partial A}{\partial x}\right), \tag{2.10}$$

and then the basic equations (2.7)–(2.9) may be rewritten as

$$\nabla^2 A = 0, \tag{2.11}$$

$$\frac{\mathrm{d}A}{\mathrm{d}t} \equiv \frac{\partial A}{\partial t} + \boldsymbol{v}_1 \cdot \nabla A = 0, \tag{2.12}$$

$$\frac{\mathrm{d}\boldsymbol{v}_1}{\mathrm{d}t} \times \nabla A = 0. \tag{2.13}$$

Now, in principle, the way of solving the set of equations (2.7)–(2.9) or (2.11)–(2.13) is as follows. First, an accessible set of potential solutions to (2.7) or (2.11), which preserve the magnetic topology, is obtained. Next, the flow speed normal to the magnetic field ($v_{1\perp}$) is determined by (2.8) or (2.12). Finally, the speed along the field ($v_{1\parallel}$) is given by solving (2.9) or (2.13). This is the hardest step since (2.9) and (2.13) are nonlinear equations which usually require a numerical

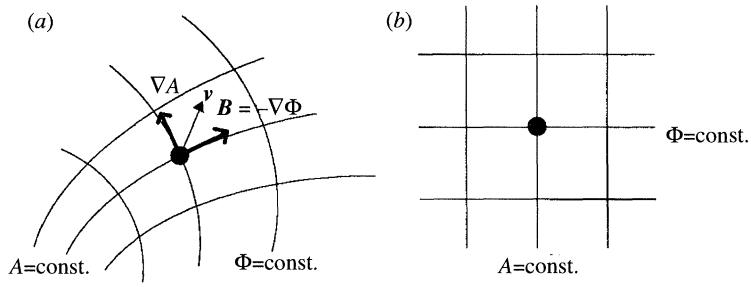

Figure 3. Contours of constant flux function A (field lines) and magnetic potential Φ in: (a) the z-plane; and (b) the f-plane, where $z = x + \mathrm{i}y$ and $f = A + \mathrm{i}\Phi$.

solution. In the next section, therefore, we develop a technique for producing a wide class of particular analytical solutions.

(b) *Frozen magnetic potential*

We introduce the magnetic potential Φ (figure 3) such that

$$(B_{0x}, B_{0y}) = \left(-\frac{\partial \Phi}{\partial x}, -\frac{\partial \Phi}{\partial y}\right), \tag{2.14}$$

and then, by comparing with (2.10), we can see that A and Φ are conjugate harmonic functions satisfying the Cauchy–Riemann equations

$$\frac{\partial \Phi}{\partial x} = -\frac{\partial A}{\partial y}, \quad \frac{\partial \Phi}{\partial y} = \frac{\partial A}{\partial x}. \tag{2.15}$$

Magnetic field lines are curves of $A = \text{const.}$, so that the vector ∇A normal to such curves is perpendicular to $\nabla \Phi$, and both A and Φ satisfy Laplace's equation.

Condition (2.12) implies that values of A are frozen to the plasma and lines of A move with it. At any one time, a given plasma element lies on the intersection of a curve $A = \text{const.}$ and a curve $\Phi = \text{const.}$, but, in general, as the plasma element moves, although its value of A is preserved, it will move along the line $A = \text{const.}$ to different values of Φ. We now assume that Φ is also frozen to the plasma, so that plasma elements preserve both A and Φ as they move. This is a key assumption of the solution that we develop in this section and generalize in § 5, although a numerical method for finding solutions with unfrozen Φ is developed in § 6. In view of the paucity of previous solutions with current sheets, the fact that we are able to obtain a whole new family of solutions with Φ frozen to the plasma is sufficient justification for adopting this assumption. However, it is shown in § 3 a that the physical consequences of this assumption are that: the current density at each point in space remains constant in time; the total current inside the current sheet is conserved; and the flow components v_x and v_y are conjugate harmonic functions satisfying Laplace's equation.

The complex function $f = A + \mathrm{i}\Phi$ may therefore be defined and, whereas in the z-plane plasma elements move around attached to a grid of curves $A = \text{const.}$ and $\Phi = \text{const.}$, in the f-plane the plasma elements remain stationary (figure 3). Our aim is then to find the mapping $f(z, t)$ and the inverse mapping $z(f, t)$.

The key equation that we need to solve is (2.9) or (2.13). However, the vector position $\boldsymbol{R} = x\hat{\boldsymbol{x}} + y\hat{\boldsymbol{y}}$ of a plasma element may be regarded as a function $\boldsymbol{R} = \boldsymbol{R}(A, \Phi, t)$ and, since the curves of $A = \text{const.}$ and $\Phi = \text{const.}$ are perpendicular,

the magnetic field $\boldsymbol{B}_0$ is in the same direction as $\partial \boldsymbol{R}/\partial \Phi$. Thus, (2.9) may be rewritten

$$\frac{\mathrm{d}^2 \boldsymbol{R}}{\mathrm{d}t^2} \cdot \frac{\partial \boldsymbol{R}}{\partial \Phi} = 0, \tag{2.16}$$

or, in terms of the complex function $z(f,t)$,

$$\left(\frac{\partial^2 z/\partial t^2}{\partial z/\partial f}\right) - \overline{\left(\frac{\partial^2 z/\partial t^2}{\partial z/\partial f}\right)} = 0, \tag{2.17}$$

where the overbar denotes a complex conjugate. The solution of this is (Titov & Priest 1993)

$$\frac{\partial^2 z}{\partial t^2} = \chi(t)\frac{\partial z}{\partial f}, \tag{2.18}$$

where $\chi(t)$ is an arbitrary real function.

Here we shall consider, in particular, the simplest case, namely of acceleration-free flows, for which $\chi \equiv 0$ (although in § 4 *c* we generalize the analysis to include accelerated flows). Then the solution of (2.18) becomes

$$z = z_0(f) + v_0(f)t, \tag{2.19}$$

where $z_0(f)$ and $v_0(f)$ are arbitrary functions. $z_0(f)$ represents the initial positions of plasma elements and $v_0(f)$ their initial velocities $(\partial z/\partial t)$.

As our basic initial field we shall consider the simplest X-point case, namely

$$B_{0x} = -y, \quad B_{0y} = -x, \tag{2.20}$$

for which

$$A = \tfrac{1}{2}(x^2 - y^2), \quad \text{and} \quad \Phi = xy,$$

so that the initial value of f, namely $f(z_0, 0)$, is

$$f_0 = \tfrac{1}{2}z_0^2. \tag{2.21}$$

The corresponding initial function z, namely $z(f,0)$, is

$$z_0(f) = \sqrt{2f} \tag{2.22}$$

for plasma elements in the right half-plane (and $-\sqrt{2f}$ for those in the left half-plane). In the above equations, and what follows, the variables are assumed to be dimensionless so that the dimensional magnetic field, complex function, complex variable, velocity and time are $B_\mathrm{e}B$, $B_\mathrm{e}L_\mathrm{e}f$, $L_\mathrm{e}z$, $V_\mathrm{e}v$ and $(L_\mathrm{e}/V_\mathrm{e})t$ in terms of the typical values B_e, L_e and V_e.

We also suppose that the initial plasma velocity is perpendicular to the magnetic field $\boldsymbol{v}_1 \cdot \boldsymbol{B}_0 = 0$ and has components

$$v_{1x} = \frac{\frac{1}{4}x}{x^2 + y^2}, \quad v_{1y} = -\frac{\frac{1}{4}y}{x^2 + y^2}, \tag{2.23}$$

so that the initial electric field $\boldsymbol{E}_0 = -\boldsymbol{v}_1 \times \boldsymbol{B}_0$ is uniform and has a magnitude of $\frac{1}{4}$. These components may be combined to give

$$v_{1x} + \mathrm{i}v_{1y} \equiv \frac{\partial z}{\partial t} = \frac{1}{4z_0},$$

and so the initial velocity function is

$$v_0(f) = \frac{1}{4\sqrt{2f}}. \tag{2.24}$$

With assumed forms (2.22) and (2.24), the Lagrangian solution (2.19) for the positions of plasma elements as a function of time and their initial positions (z_0) becomes

$$z = z_0 + \frac{t}{4z_0}.$$

This may be inverted to give

$$2z_0 = z + \sqrt{(z^2 - t)}, \tag{2.25}$$

so that $z = z_0$ at $t = 0$. (The negative square root gives the spurious solution $z_0 = 0$ when $t = 0$.)

Since the plasma elements preserve their values of f as they move, and initially $f = f_0$, where f_0 is given by (2.21) and z_0 by (2.25), we deduce that

$$f(z,t) = \tfrac{1}{8}(z + \sqrt{(z^2 - t)})^2, \tag{2.26}$$

which is the required function that we have been seeking. The resulting magnetic field and plasma velocity components are

$$B_{0y} + \mathrm{i}B_{0x} \equiv \mathcal{B}(z,t) = -\frac{\partial f}{\partial z} = -\frac{(z + \sqrt{(z^2 - t)})^2}{4\sqrt{(z^2 - t)}} \tag{2.27}$$

and

$$v_{1x} + \mathrm{i}v_{1y} \equiv \mathcal{V}(z,t) = \frac{\partial z}{\partial t} = \frac{1}{4z_0} = \frac{\frac{1}{2}}{z + \sqrt{(z^2 - t)}}. \tag{2.28}$$

Also, the electric field is

$$E_0 = -v_{1x}B_{0y} + v_{1y}B_{0x} = \mathrm{Re}(-\mathcal{V}B) = \tfrac{1}{8}\,\mathrm{Re}\left(\frac{z}{\sqrt{(z^2 - t)}} + 1\right), \tag{2.29}$$

which is equal to $\frac{1}{4}$ at $t = 0$, as required. In addition, the plasma density is given by

$$\rho = \frac{\rho_0}{|\partial z/\partial z_0|^2} = \frac{\rho_0}{|1 - t/(z + \sqrt{(z^2 - t)})^2|^2}, \tag{2.30}$$

which initially is assumed to be uniform ($\rho = \rho_0$). We adopt this assumption for simplicity, although in general the initial density may be non-uniform.

3. Properties of the basic solution

The magnetic field lines are shown in figure 4. A current sheet stretches along the x-axis from $z = -\sqrt{t}$ to $z = \sqrt{t}$ at time t. The ends of the sheet move outwards at a speed $1/(2\sqrt{t})$. Several interesting properties of the solution may be derived.

1. From (2.28) it can be seen that each plasma element moves at a constant velocity $1/(4z_0) = v_0(f)$ in a straight line towards the x-axis. The direction of the motion is perpendicular to the initial magnetic field and the magnitude is inversely proportional to the initial distance from the origin.

PHILOSOPHICAL TRANSACTIONS OF THE ROYAL SOCIETY A MATHEMATICAL, PHYSICAL & ENGINEERING SCIENCES

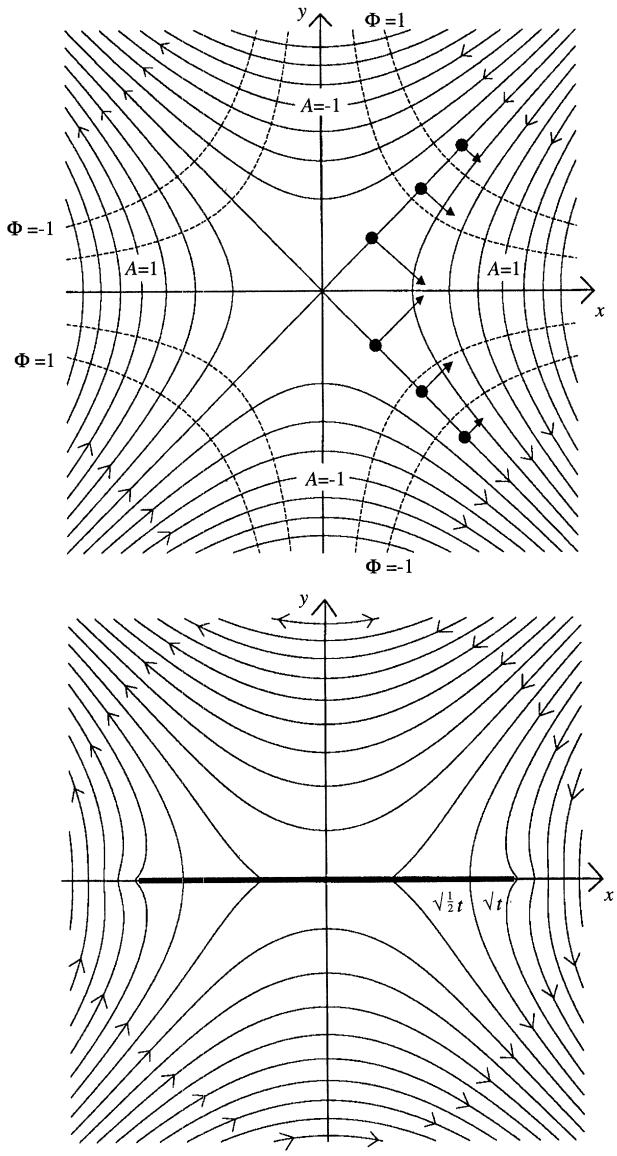

Figure 4. Magnetic field lines (solid) for: (*a*) the basic solution at $t = 0$; and (*b*) at $t > 0$ when a current sheet stretches from $z = -\sqrt{t}$ to $z = \sqrt{t}$.

2. The form (2.27) for the magnetic field components is elegant, but the separate components as functions of x and y are far from simple, and may be found by taking real and imaginary parts of (2.27) to give

$$B_{0x} = -\frac{1}{2}\left[y + \tilde{R}_- + \frac{2xy\tilde{R}_+ - (x^2 - y^2)\tilde{R}_-}{4(R_+^2 + R_-^2)}\right],$$
$$B_{0y} = -\frac{1}{2}\left[x + \tilde{R}_+ + \frac{2xy\tilde{R}_- + (x^2 - y^2)\tilde{R}_+}{4(R_+^2 + R_-^2)}\right], \tag{3.1}$$

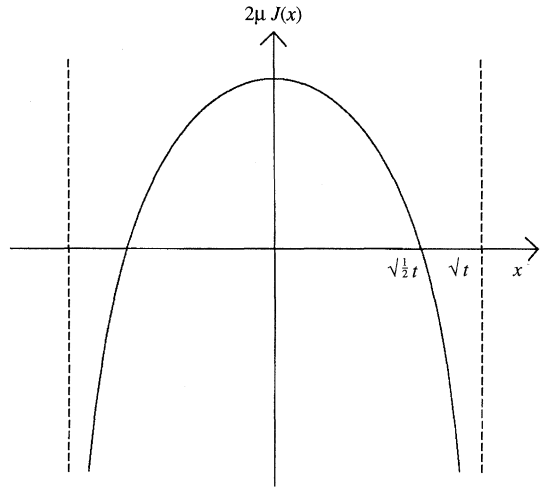

Figure 5. The current density $J(x)$ in the sheet as a function of distance x along the sheet.

where

$$R_+ = [m + (x^2 - y^2 - t)]^{1/2}/(2\sqrt{2}), \quad R_- = [m - (x^2 - y^2 - t)]^{1/2}/(2\sqrt{2}),$$
$$\tilde{R}_+ = R_+ \operatorname{sgn}(x), \quad \tilde{R}_- = R_- \operatorname{sgn}(y), \quad m = [(x^2 - y^2 - t)^2 + 4x^2y^2]^{1/2}.$$

The corresponding flux function and magnetic potential are

$$A(x, y, t) = \tfrac{1}{2}[\tfrac{1}{2}(x^2 - y^2) - \tfrac{1}{4}t + x\tilde{R}_+ - y\tilde{R}_-] \tag{3.2}$$

and

$$\Phi(x, y, t) = \tfrac{1}{2}(xy + x\tilde{R}_- + y\tilde{R}_+).$$

Similarly, the real and imaginary parts of (2.28) give the velocity components as

$$v_{1x} = \frac{\frac{1}{2}x + \tilde{R}_+}{4[(\frac{1}{2}x + \tilde{R}_+)^2 + (\frac{1}{2}y + \tilde{R}_-)^2]}, \tag{3.3}$$
$$v_{1y} = \frac{-\frac{1}{2}y - \tilde{R}_-}{4[(\frac{1}{2}x + \tilde{R}_+)^2 + (\frac{1}{2}y + \tilde{R}_-)^2]}.$$

3. The solutions $A(z, t)$, $\mathcal{B}(z, t)$, $\mathcal{V}(z, t)$ are self-similar since they may be written in the form $G(t)H(z/\sqrt{t})$.

4. At the sheet ($y = 0$, $x^2 < t$), there is a normal component

$$B_{0y} = -\tfrac{1}{2}x, \tag{3.4}$$

which is continuous across the sheet and is exactly half of the initial value (2.20). Thus, as the sheet grows in length, it swallows up half of the magnetic flux, while the remainder piles up ahead of it. The tangential component of the field at the sheet is

$$B_{0x} = \pm\frac{1}{4}\left[\frac{x^2}{(t - x^2)^{1/2}} - (t - x^2)^{1/2}\right], \tag{3.5}$$

where the plus and minus signs refer to the values above and below the sheet,

respectively. On the top side of the sheet, B_{0x} is negative for $|x| < \sqrt{(\frac{1}{2}t)}$ and positive for $\sqrt{(\frac{1}{2}t)} < x < \sqrt{t}$. At $x = \sqrt{(\frac{1}{2}t)}$, the field is normal to the sheet.

5. The current density of the sheet is

$$J(x) = -\frac{(B_{0x})_{y=0+} - (B_{0x})_{y=0-}}{\mu},$$

and so from (2.35) it has the form

$$J(x) = \frac{1}{\mu}\left[\frac{\frac{1}{2}t - x^2}{(t-x^2)^{1/2}}\right], \tag{3.6}$$

as sketched in figure 5. The current reverses sign at $\pm\sqrt{(\frac{1}{2}t)}$, so that the ends of the sheet possess regions of reversed current. The current at the centre of the sheet grows in time like $\sqrt{t}$.

6. Now, what about the rate of magnetic energy dissipation? First, let us calculate the Poynting flux P of magnetic energy into the sheet, around a contour C which encircles the sheet, namely

$$\begin{aligned} -\oint_C \frac{B_0^2}{\mu} v_n \, ds &= -\oint_C \frac{\mathcal{B}\bar{\mathcal{B}}}{\mu} \operatorname{Im}(\bar{\mathcal{V}}\, dz) \\ &= -\oint_{C_0} \frac{\mathcal{B}_0\bar{\mathcal{B}}_0}{\mu \partial z/\partial z_0 \, \overline{\partial z/\partial z_0}} \operatorname{Im}\left(\bar{\mathcal{V}}_0 \frac{\partial z}{\partial z_0} dz_0\right), \end{aligned} \tag{3.7}$$

where

$$\mathcal{B}_0\bar{\mathcal{B}}_0 = z_0\bar{z}_0 = \tfrac{1}{4}t, \quad \frac{\partial z}{\partial z_0} = 1 - \frac{t}{4z_0^2}$$

and the contour C_0 in the z_0 plane is a circle of radius $\sqrt{t}/2$ given by $z_0 = \sqrt{t}/2 \exp(i\alpha)$, say. Then

$$\frac{\partial z}{\partial z_0}\overline{\frac{\partial z}{\partial z_0}} = 2(1 - \cos 2\alpha)$$

and

$$\operatorname{Im}\left(\bar{\mathcal{V}}_0 \frac{\partial z}{\partial z_0} dz_0\right) = \tfrac{1}{4}(\cos 2\alpha - 1)\, d\alpha,$$

so that (3.7) reduces simply to

$$P = \frac{t}{32\mu}\int_0^{2\pi} d\alpha = \frac{\pi t}{16\mu}. \tag{3.8}$$

In other words, the flux of magnetic energy into the sheet grows linearly in time as the sheet lengthens. However, since the sheet has zero width in the present model, it contains zero magnetic energy, and, by Poynting's theorem, P represents the rate at which energy is being converted. Typically half goes into ohmic heating and half into the work done by the Lorentz force, the exact proportions depending on the details of the current-sheet interior.

7. In setting up our expansion in the form (2.6), we have assumed that the flow speed exceeds the sound speed and is smaller than the Alfven speed. We may now therefore estimate *a posteriori* the region of validity of these approximations

PHILOSOPHICAL TRANSACTIONS OF THE ROYAL SOCIETY A MATHEMATICAL, PHYSICAL & ENGINEERING SCIENCES

in terms of the initial positions z_0 of the plasma elements. First, we find that in dimensional variables

$$\tfrac{1}{2}\sqrt{\frac{v_e}{v_{Ae}}} < \frac{|z_0|}{L_e} < \frac{v_e}{4c_{se}}, \tag{3.9}$$

which fails at small values of z_0 where the flow speed becomes too large and at large values of z_0 where the flow speed becomes too small. In addition, near the ends of the current sheet where $2z_0/\sqrt{(L_e v_e)} = \pm\sqrt{t}$, the sound speed becomes too large, giving the extra condition that

$$\left(\frac{2z_0}{\sqrt{(L_e v_e)}} \pm \sqrt{t}\right) > \frac{1}{2}\sqrt{t}\left(\frac{4tv_e/L_e}{v_e^2/c_{se}^2}\right)^{1/(2(\gamma-1))}. \tag{3.10}$$

(*a*) *A current conservation theorem*

A rather surprising feature of basic solution (2.27) is that the total current in the sheet, obtained by integrating (3.6) between $-\sqrt{t}$ and $+\sqrt{t}$, vanishes so that the positive and negative contributions cancel out. This may also be seen from the fact that there is no current outside the sheet and the field (2.27) at large distances has the form

$$-z + \frac{c}{z} + O\left(\frac{1}{z^3}\right),$$

with $c = 0$ so that the line-current contribution vanishes.

So why does the current vanish? Basically, it is because of the nature of the flows being considered and, in particular, the assumption that Φ is conserved, as shown in the following theorem.

Theorem. *The total current I in a sheet, which forms by collapse of an initially current-free X-point, vanishes under the strong magnetic field approximation if the flux function A and magnetic potential Φ are conserved.*

Proof. The total current in the sheet is

$$I = \oint \boldsymbol{B}_0 \cdot \mathrm{d}\boldsymbol{s},$$

evaluated along a circuit encircling the sheet. This may be written in complex-variable notation as

$$I = \mathrm{Im} \oint \mathcal{B}(z)\,\mathrm{d}z$$

or, from the definition of $\mathcal{B}$ in terms of the complex potential $f(z)$,

$$I = -\,\mathrm{Im} \oint \frac{\mathrm{d}f}{\mathrm{d}z}\mathrm{d}z = -\,\mathrm{Im} \oint \mathrm{d}f.$$

But, if A and Φ are conserved, $f = f_0$ and so

$$I = -\,\mathrm{Im} \oint \mathrm{d}f_0.$$

However, in the initial state, there is no current and so

$$I = 0,$$

as required. ■

Thus, the conservation of current is a rather general property of a wide class of flows and initial states and is not restricted to the particular basic solution we have discovered. In particular, it will hold for: other initial states and not just (2.21); other initial velocities and not just (2.24); and other solutions to basic equation (2.18) for $z(f,t)$ and not just the acceleration-free solution (2.19).

Several other comments concerning the consequences of Φ being frozen to the plasma may be made. First note that, if the magnetic field is written in terms of the magnetic potential Φ, the current enclosed by a circuit may be written

$$I = \oint \boldsymbol{B}_0 \cdot \mathrm{d}\boldsymbol{s} = \int \nabla\Phi \cdot \mathrm{d}\boldsymbol{s} = \int \mathrm{d}\Phi. \tag{3.11}$$

Of course, if the magnetic field is current-free along the circuit, in general this does not necessarily vanish – see, for example, the potential $\Phi = \phi$ of a point source. However, if Φ is single-valued then the current does vanish. It can be seen that our solution (2.26) for f (and therefore Φ) is indeed single-valued. But, for example, (1.10) has

$$f = -\tfrac{1}{2}z(z^2 + L^2)^{1/2} + \tfrac{1}{2}L^2 \sinh^{-1}(z/L),$$

which is not single-valued.

If Φ is frozen to the plasma,

$$\frac{\partial\Phi}{\partial t} + \boldsymbol{v}_1 \cdot \nabla\Phi = 0, \tag{3.12}$$

or, from definition (2.14) of Φ,

$$\frac{\partial\Phi}{\partial t} - \boldsymbol{v}_1 \cdot \boldsymbol{B}_0 = 0.$$

Taking the gradient and again using (2.14) we find

$$\frac{\partial \boldsymbol{B}_0}{\partial t} = -\nabla(\boldsymbol{v}_1 \cdot \boldsymbol{B}_0). \tag{3.13}$$

This equation has several consequences. The first, by taking the curl, is

$$\frac{\partial}{\partial t}(\nabla \times \boldsymbol{B}_0) = 0, \tag{3.14}$$

so that the current remains constant in time at each point. The second, by taking the divergence, is that

$$\nabla^2(\boldsymbol{v}_1 \cdot \boldsymbol{B}_0) = 0, \tag{3.15}$$

so that $\boldsymbol{v}_1 \cdot \boldsymbol{B}_0$ is harmonic. Third, by subtracting from (2.2), we obtain

$$\nabla(\boldsymbol{v}_1 \cdot \boldsymbol{B}_0) + (\boldsymbol{B}_0 \cdot \nabla)\boldsymbol{v}_1 - (\nabla \cdot \boldsymbol{v}_1)\boldsymbol{B}_0 - (\boldsymbol{v}_1 \cdot \nabla)\boldsymbol{B}_0 = 0.$$

The x- and y-components of this equation reduce to

$$B_{0y}\left(\frac{\partial v_{1y}}{\partial x} + \frac{\partial v_{1x}}{\partial y}\right) = \left(\frac{\partial v_{1y}}{\partial y} - \frac{\partial v_{1x}}{\partial x}\right) B_{0x},$$

$$B_{0x}\left(\frac{\partial v_{1y}}{\partial x} + \frac{\partial v_{1x}}{\partial y}\right) = \left(\frac{\partial v_{1x}}{\partial x} - \frac{\partial v_{1y}}{\partial y}\right) B_{0y},$$

PHILOSOPHICAL TRANSACTIONS OF THE ROYAL SOCIETY A MATHEMATICAL, PHYSICAL & ENGINEERING SCIENCES

which implies that

$$\frac{\partial v_{1y}}{\partial x} = -\frac{\partial v_{1x}}{\partial y} \quad \text{and} \quad \frac{\partial v_{1y}}{\partial y} = \frac{\partial v_{1x}}{\partial x}. \tag{3.16}$$

In other words, v_{1x} and v_{1y} are conjugate harmonic functions satisfying Laplace's equation. (This is consistent of course with our earlier result that $v_{1x} + \mathrm{i}v_{1y}$ is analytic (2.28).)

4. Generalizations of the basic solution

In deriving our basic solution (2.26) for the complex potential $f(z,t)$ from the acceleration-free solution (2.19) for $z(f,t)$ to the basic equation (2.18), we have assumed an initial X-point field $f_0 = \frac{1}{2}z_0^2$ (2.21), which determined the arbitrary function $z_0(f)$ as its inverse. In addition, the second arbitrary function $v_0(f)$ was determined from the condition that

$$v_0(f)z_0(f) = \tfrac{1}{4}. \tag{4.1}$$

Since in this case $z_0 = \partial f_0/\partial t \equiv -\mathcal{B}_0$, the initial flow is perpendicular to the magnetic field (because $\mathcal{V}_0\mathcal{B}_0$ is real), and the initial electric field is $\frac{1}{4}$.

(a) *Line current source*

Now let us examine the consequences of picking other initial functions f_0 which have previously been discussed in the literature in relation to important physical problems. For example, the function

$$f_0(z) = \frac{\mu I}{2\pi}\log z \tag{4.2}$$

gives a flux function and magnetic field

$$A = \frac{\mu I}{2\pi}\log r, \quad B_{0\theta} \equiv -\frac{\partial A}{\partial r} = -\frac{\mu I}{2\pi r}.$$

It represents the configuration with circular field lines created by a line current at the origin (figure 6*a*) having the equations $\log\sqrt{x^2+y^2} = \text{const.}$, which is commonly invoked in plasma physics as a model for a magnetic field produced by a line source. The inverse function is

$$z_0(f) = \mathrm{e}^{2\pi f/(\mu I)}, \tag{4.3}$$

and so, if we again use condition (4.1), the initial velocity is

$$v_0(f) = \tfrac{1}{4}\mathrm{e}^{-2\pi f/(\mu I)}. \tag{4.4}$$

The resulting Lagrangian form of the positions (z) of plasma elements in terms of their initial values (z_0) is the same as before, namely (2.24), and so the inverse solution is again given by

$$2z_0 = z + \sqrt{(z^2 - t)}. \tag{4.5}$$

Since the values of f are preserved following plasma elements, $f = f_0$, where f_0 is given by (4.2) and z_0 by (4.5), so that

$$f(z,t) = \frac{\mu I}{2\pi}\log[\tfrac{1}{2}(z + \sqrt{(z^2 - t)})]. \tag{4.6}$$

PHILOSOPHICAL TRANSACTIONS OF THE ROYAL SOCIETY A MATHEMATICAL, PHYSICAL & ENGINEERING SCIENCES

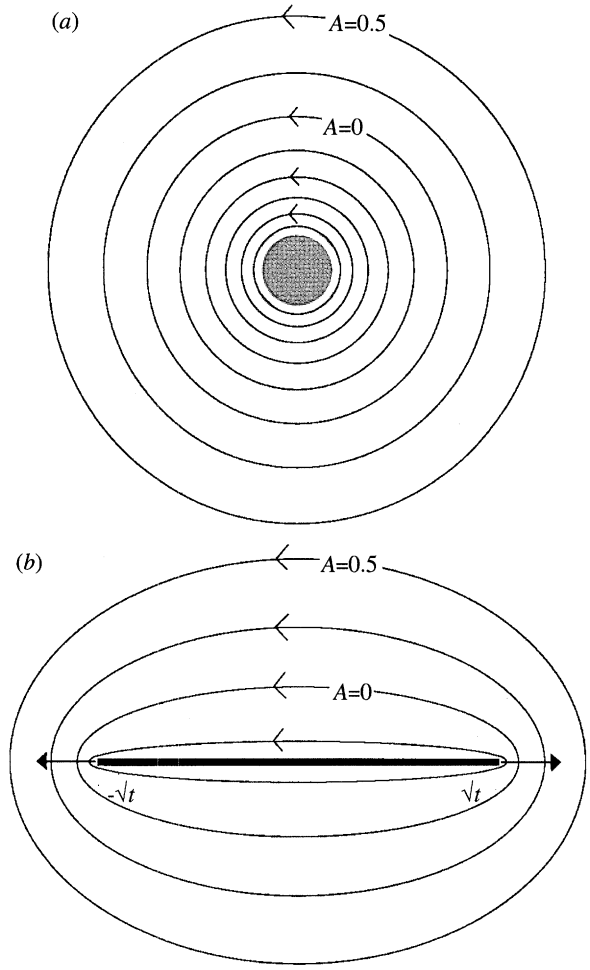

Figure 6. Magnetic field lines for: (a) a current filament; that (b) splits into a current sheet.

The resulting magnetic field is

$$B_{0y} + \mathrm{i}B_{0x} \equiv -\frac{\partial f}{\partial z} = -\frac{\mu I}{2\pi\sqrt{(z^2 - t)}}. \tag{4.7}$$

Initially it gives the field $-\mu I/(2\pi z)$, and, as time proceeds, the current filament splits into a current sheet of length $2\sqrt{t}$, stretching from $z = -\sqrt{t}$ to $z = \sqrt{t}$ (figure 6*b*). The field lines are given by $\log\sqrt{[(\frac{1}{2}x + R_+)^2 + (\frac{1}{2}y + R_-)^2]} = \text{const}$. The plasma velocity is

$$v_{1x} + \mathrm{i}v_{1y} \equiv \frac{\partial z}{\partial t} = \frac{1}{4z_0} = \frac{\frac{1}{2}}{z + \sqrt{(z^2 - t)}}. \tag{4.8}$$

From (4.7), the magnetic field components are given by

$$2B_{0x}^2 = \left(\frac{\mu I}{2\pi}\right)^2 \frac{-X + \sqrt{(X^2 + 4Y^2)}}{(X^2 + 4Y^2)}, \quad 2B_{0y}^2 = \left(\frac{\mu I}{2\pi}\right)^2 \frac{X + \sqrt{(X^2 + 4Y^2)}}{(X^2 + 4Y^2)}, \tag{4.9}$$

where $X = x^2 - y^2 - t$, $Y = xy$. In particular, on the current sheet ($y = 0$, $x^2 < t$),

B_y vanishes and

$$B_{0x} = \frac{\mu I}{2\pi\sqrt{(t-x^2)}},$$

with B_{0x} jumping from a positive value below to a negative value above the sheet. Thus, the current density in the sheet has a magnitude

$$J(x) = \frac{I}{\pi\sqrt{(t-x^2)}}. \tag{4.10}$$

Integrating this from one end of the sheet to the other, we find that the total current in the sheet is I, and therefore conserved in time, as we expect from our current conservation theorem.

The initial flow and electric field are different in form from the basic solution (2.26). The initial streamlines are those of a hyperbolic flow coming in along the y-axis and out along the x-axis and are only perpendicular to the magnetic field along the x- and y-axes. The initial electric field is not uniform but is $\mu I(x^2 - y^2)/[8\pi(x^2+y^2)^2]$.

(*b*) *Two line-current sources*

A second example is to start with the complex potential

$$f_0(z) = \log(z^2 - a_0^2), \tag{4.11}$$

due to two line sources at $z = a_0$ and $z = -a_0$ (figure 7*a*), which is of great historical interest since it was the example considered by Green (1965) when first modelling current-sheet creation in astrophysics. The inverse function is

$$z_0(f) = \sqrt{(a_0^2 + e^f)}, \tag{4.12}$$

and, by imposing an initial velocity of the form

$$v_0(f) = -\frac{1}{4\sqrt{(a_0^2+e^f)}}, \tag{4.13}$$

we find

$$z = z_0 - \frac{t}{4z_0}, \tag{4.14}$$

with an inverse solution given by

$$2z_0 = z + \sqrt{(z^2+t)}, \tag{4.15}$$

which is of the same form as (4.5) except that t is replaced by $-t$. As usual, since f remains constant following plasma elements, the solution for $f(z,t)$ is given by (4.11) with z_0 from (4.15), namely

$$f = \log(2z^2 + t + 2z\sqrt{(z^2+t)} - 4a_0^2) - \log 4. \tag{4.16}$$

The corresponding complex magnetic field is

$$B_{0y} + \mathrm{i}B_{0x} = -\frac{\partial f}{\partial z} = -\frac{4z^2 + 2t + 4z\sqrt{(z^2+t)}}{\sqrt{(z^2+t)}(2z^2 + t - 4a_0^2 + 2z\sqrt{(z^2+t)})}. \tag{4.17}$$

This approaches the form $-2z/(z^2 - a_0^2)$, corresponding to (4.11), as t tends to zero. It has a current sheet stretching from $z = -\mathrm{i}\sqrt{t}$ to $\mathrm{i}\sqrt{t}$ and the sources that

PHILOSOPHICAL TRANSACTIONS OF THE ROYAL SOCIETY A MATHEMATICAL, PHYSICAL & ENGINEERING SCIENCES

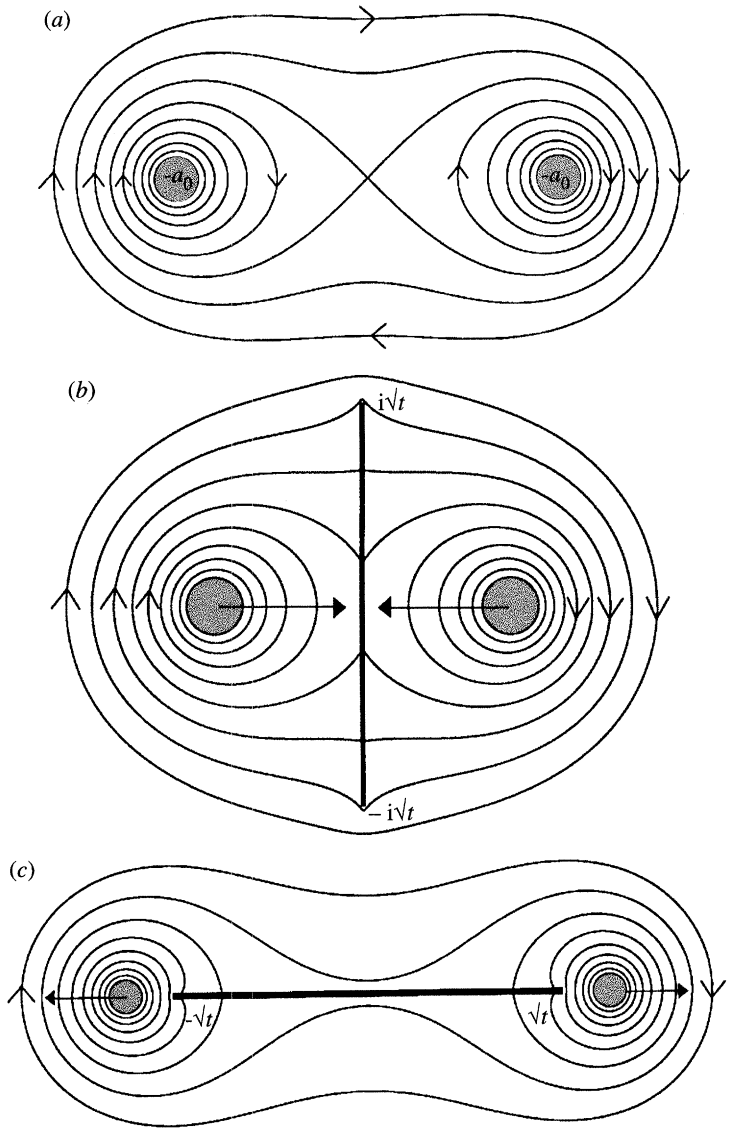

Figure 7. Magnetic field lines for (a) a pair of line-current sources that create a current sheet by: (b) converging; and (c) diverging motions.

were initially at $z = \pm a_0$ have moved with constant speeds of $\mp 1/(4a_0)$ to the locations $z = a_0 - t/(4a_0)$ and $z = -a_0 + t/(4a_0)$, as shown in figure 7*b*.

If, instead of (4.13), the initial velocity

$$v_0(f) = \frac{1}{4\sqrt{(a_0^2 + e^f)}} \tag{4.18}$$

is assumed, the effect is to replace t by $-t$ in the above solution (4.14)–(4.17), so that a current sheet stretches from $z = -\sqrt{t}$ to $z = \sqrt{t}$ and the sources move to $z = a_0 + t/(4a_0)$ and $z = -a_0 - t/(4a_0)$. The resulting current sheet formed by sources moving apart at constant speeds is shown in figure 7*c*.

(c) Two dipole sources

A third example is to consider the potential

$$f_0(z) = \frac{-2\mathrm{i}Dz}{z^2 - a_0^2}, \tag{4.19}$$

which is of great interest in a solar context. It represents the coronal field due to two collinear bipolar regions at $z = \pm a_0$ (figure 8*a*), and was used to model solar flares by Priest and Raadu (1975). More recently, it has been invoked as an important example of solar coronal heating by the interaction of neighbouring bipolar flux regions. The required inverse function is

$$z_0(f) = \frac{\mathrm{i}}{f}[-D + \sqrt{(D^2 - a_0^2 f^2)}]. \tag{4.20}$$

For the initial flow function we choose

$$v_0(f) = -\frac{1}{4(z_0 - \mathrm{i}a_0)} + \frac{\mathrm{i}}{8a_0}, \tag{4.21}$$

which has the property of being a potential stagnation-point flow centred about the X-point ($z_0 = \mathrm{i}a_0$) of the initial field, together with a uniform upflow which ensures that the dipole sources move along the x-axis towards one another.

The Lagrangian solution for the positions of plasma elements is then

$$z = z_0 - \frac{t}{4(z_0 - \mathrm{i}a_0)} + \frac{\mathrm{i}t}{8a_0}, \tag{4.22}$$

and its inverse is given by

$$2z_0 = z + \mathrm{i}\left(a_0 - \frac{t}{8a_0}\right) + \sqrt{\left[z - i\left(a_0 + \frac{t}{8a_0}\right)\right]^2 + t}. \tag{4.23}$$

The resulting solution for f is found by putting $f = f_0$, where f_0 is given by (4.19) and z_0 by (4.23), namely

$$\begin{aligned} f(z,t) = -2\mathrm{i}D\Bigg\{ & z + \mathrm{i}\left(a_0 - \frac{t}{8a_0}\right) + \left\{\left[z - \mathrm{i}\left(a_0 + \frac{t}{8a_0}\right)\right]^2 + t\right\}\Bigg\} \\ & \times\left\{z^2 - \frac{\mathrm{i}tz}{4a_0} - 3a_0^2 - \frac{t^2}{64a_0^2} + \frac{t}{2} + \left[z + \mathrm{i}\left(a_0 - \frac{t}{8a_0}\right)\right]\right. \\ & \left.\times\left\{\left[z - \mathrm{i}\left(a_0 + \frac{t}{8a_0}\right)\right]^2 + t\right\}^{1/2}\right\}^{-1}. \end{aligned} \tag{4.24}$$

As time increases, the dipole sources approach one another at a constant relative speed of $\frac{1}{4}a_0^{-1}$, and are located at $z = \pm[a_0 - t/(8a_0)]$. The current sheet grows and rises, with its ends at the points $z = \mathrm{i}[a_0 + t/(8a_0) \pm \sqrt{t}]$, so that its length at time t is $2\sqrt{t}$.

If, in place of (4.21), an initial flow of

$$v_0(f) = \frac{1}{4(z_0 - \mathrm{i}a_0)} + \frac{\mathrm{i}t}{8a_0}$$

is assumed, then the dipole sources instead separate and a curved current sheet

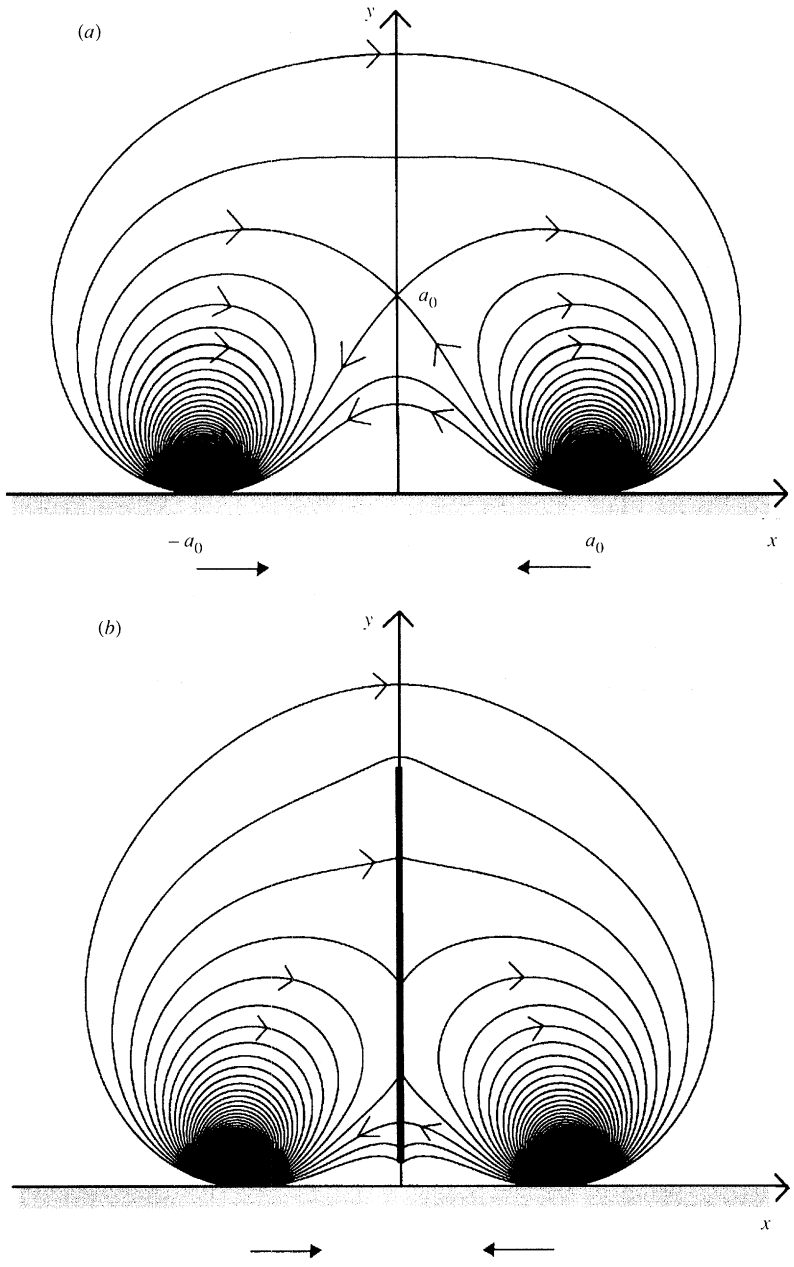

Figure 8. The magnetic field due (*a*) a pair of dipoles which (*b*) approach and create a current sheet.

is formed with its end-points at

$$z = \mathrm{i}\left(a_0 + \frac{t^2}{8a_0}\right) \pm \sqrt{t}.$$

The evolution of a current sheet between unequal dipole sources may also be modelled, following the approach of Tur & Priest (1976).

PHILOSOPHICAL TRANSACTIONS OF THE ROYAL SOCIETY A MATHEMATICAL, PHYSICAL & ENGINEERING SCIENCES

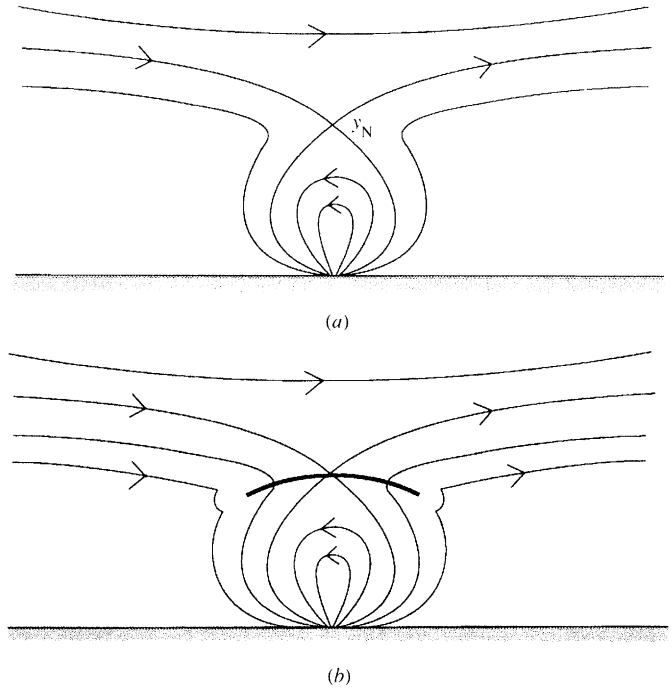

Figure 9. A sketch of the magnetic field lines due to (*a*) a dipole and a uniform field which (*b*) interact and create a current sheet.

(*d*) *Flux emergence*

Tur & Priest (1976) have suggested that the emergence of new flux from below the solar photosphere and its interaction with an overlying horizontal coronal magnetic field may be modelled by means of the potential

$$f_0(z) = \mathrm{i}B_0\left(-z + \frac{y_N^2}{z}\right). \tag{4.25}$$

This represents a horizontal field of strength B_0, together with a dipole of strength $B_0 y_N^2$ placed at the origin. Flux emergence is a fundamental process in the Sun and other stars, and also in accretion discs, and so it is important to study the consequences of flux emergence for heating the overlying coronae. The field contains an X-point at $z_0 = \mathrm{i}y_N$ (figure 9). The analysis of the present paper may therefore be followed by first noting that the required inverse function is

$$z_0(f) = \mathrm{i}\frac{f}{2B_0} + \sqrt{y_N^2 - \frac{f^2}{4B_0^2}}.$$

For the initial flow function we then assume

$$v_0(f) = \frac{1}{4(z_0 - \mathrm{i}y_N)} + \frac{1}{4\mathrm{i}y_N},$$

which represents a stagnation-point flow about the X-point together with a uniform vertical motion which keeps the dipole source at a fixed location.

The positions z of plasma elements initially at z_0 are then given by

$$z = z_0 + \frac{t}{4(z_0 - \mathrm{i}y_\mathrm{N})} + \frac{t}{4\mathrm{i}y_\mathrm{N}},$$

which gives the inverse solution as

$$2z_0 = z + \frac{\mathrm{i}t}{4y_\mathrm{N}} + \mathrm{i}y_\mathrm{N} + \sqrt{\left[\left(z + \frac{\mathrm{i}t}{4y_\mathrm{N}} - \mathrm{i}y_\mathrm{N}\right)^2 - t\right]}. \tag{4.26}$$

By putting $f = f_0$ and substituting for f_0 and z_0 from (4.25) and (4.26), the resulting solution for the complex potential is

$$\begin{aligned} f(z,t) = \tfrac{1}{2}\mathrm{i}B_0 \Bigg\{ & 6y_\mathrm{N}^2 - 2z^2 + \frac{t^2}{8y_\mathrm{N}^2} + t - \frac{\mathrm{i}tz}{y_\mathrm{N}} - 2\left(z + \frac{\mathrm{i}t}{4y_\mathrm{N}} + \mathrm{i}y_\mathrm{N}\right) \\ & \times \left[\left(z + \frac{\mathrm{i}t}{4y_\mathrm{N}} - \mathrm{i}y_\mathrm{N}\right)^2 - t\right]^{1/2} \Bigg\} \\ & \times \left[z + \frac{\mathrm{i}t}{4y_\mathrm{N}} + \mathrm{i}y_\mathrm{N} + \sqrt{\left(z + \frac{\mathrm{i}t}{4y_\mathrm{N}} - \mathrm{i}y_\mathrm{N}\right)^2 - t}\right]^{-1}. \end{aligned} \tag{4.27}$$

The ends of the current sheet which grows in time are therefore located at $z = \mathrm{i}y_\mathrm{N} - \frac{1}{4}\mathrm{i}t/y_\mathrm{N} \pm \sqrt{t}$. In this model, due to an upward flow at the photospheric level, the magnetic field lines rise up and reach the current sheet where they reconnect, so that the lower part of them (with respect to the sheet) is accumulated near the dipole source. Indeed, we have from above

$$\left.\frac{\partial z}{\partial z_0}\right|_{z_0=0} = 1 + \frac{t}{4y_N^2},$$

and, hence, near the dipole

$$z_0 \simeq \frac{z}{(1 + (t/4y_N^2))},$$

so from (4.25) if follows that

$$f \simeq \mathrm{i}B_0 \left[-\frac{z}{(1 + t/(4y_N^2))} + \frac{y_N^2(1 + t/(4y_N^2))}{z}\right],$$

which demonstrates the increase of the dipole moment in time.

(*e*) *Four line currents*

The interaction of a quadrupolar magnetic structure consisting of four magnetic islands surrounding an X-point was considered numerically by Bajer (1990). An elegant model having a similar qualitative form to his may be set up by considering the initial complex potential

$$f_0(z) = \log \frac{z^2 - a_0^2}{z^2 + a_0^2}, \tag{4.28}$$

which is due to four line currents of equal magnitude at $z = \pm a_0, \pm \mathrm{i}a_0$ such that adjacent line currents have opposite directions (figure 10). The required inverse

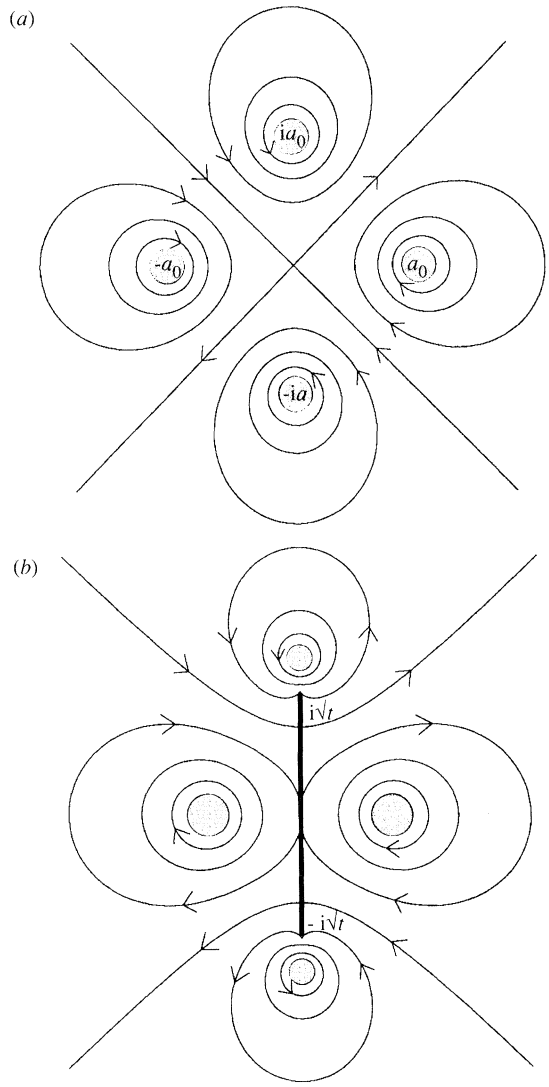

Figure 10. Sketch of the magnetic field of four line currents that move and create a current sheet.

function is

$$z_0(f) = a_0 \left(\frac{1 + e^f}{1 - e^f} \right)^{1/2}$$

and the initial flow function $v_0 = -\frac{1}{4} z_0^{-1}$ leads, as usual, to the relation

$$2z_0 = z + \sqrt{(z^2 + t)}. \tag{4.29}$$

Writing $f = f_0$, and substituting for z_0 from (4.29), we therefore find the solution

$$f(z,t) = \log \frac{[z + \sqrt{(z^2 + t)}]^2 - 4a_0^2}{[z + \sqrt{(z^2 + t)}]^2 + 4a_0^2}. \tag{4.30}$$

PHILOSOPHICAL TRANSACTIONS OF THE ROYAL SOCIETY A MATHEMATICAL, PHYSICAL & ENGINEERING SCIENCES

This has branch points, the ends of the current sheet, at $z = \pm \mathrm{i}\sqrt{t}$, which move apart in time. The sources have moved to the locations where the argument of the logarithm is either zero or infinite, namely

$$z = \pm \left(a_0 - \frac{t}{4a_0} \right) \quad \text{and} \quad z = \pm \mathrm{i} \left(a_0 + \frac{t}{4a_0} \right).$$

Thus, the two sources originally at $z = \pm a_0$ approach one another at a relative speed of $1/(2a_0)$, while those at $\pm \mathrm{i}a_0$ move apart at the same speed. The solution may be modified to give a structure of four lobes within a closed circular field line at $r = 1$, say, by considering

$$f_0(z) = \log \frac{(z^2 - a_0^2)(a_0^2 z^2 + 1)}{(z^2 + a_0^2)(a_0^2 z^2 - 1)}$$

in place of (4.28). This is even closer to Bajer's model.

(*f*) *Initial velocity*

When deriving our basic solution (2.26), we assumed an initial velocity function

$$v_0 \equiv v_{1x} + \mathrm{i} v_{1y} = \frac{1}{4z_0} \tag{4.31}$$

and substituted it into the general solution

$$z = z_0 + v_0 t \tag{4.32}$$

before inverting to find $z_0 = z_0(z, t)$ (2.25). There is, however, very little choice in the form of this velocity function. Replacing (4.31) by

$$v_0 = \frac{c^2}{z_0} \tag{4.33}$$

simply has the effect of replacing t in (4.32) and (2.26) by $4c^2 t$, so that the current sheet stretches between $z = -2c\sqrt{t}$ and $z = 2c\sqrt{t}$. A velocity function of $v_0 = -c^2/z_0$, on the other hand, makes the current sheet grow in the y-direction and stretch between $z = -2\mathrm{i}c\sqrt{t}$ and $z = 2\mathrm{i}c\sqrt{t}$.

What are the constraints on the form of v_0? First, except at the origin, it needs to be an analytic function of z when the magnetic potential is frozen-in, as shown in § 3 *a*. Second, the flow needs to look qualitatively like that of (4.31) with the field lines being carried in along the y-axis, say, to form the sheet, and out along the x-axis, say. Third, since the electric field is initially

$$E_0 = -\operatorname{Re}(\mathcal{V}_0 \mathcal{B}_0),$$

and $\mathcal{B}_0 = -z_0$, if it is to be non-zero at the origin then v_0 must have a singularity at least as strong as z_0^{-1}.

Now, an analytic function which is regular in a finite region $0 < |z| < R$ outside the origin can always be expanded in a Laurent series

$$\sum_{n=0}^{\infty} a_n z^n + \sum_{n=1}^{\infty} b_n z^{-n}.$$

Thus, we see that the form (4.31) is simply the first term in the part of the series with negative powers and it initially makes the electric field constant and the flow

perpendicular to the field. The positive powers of z do not provide the required form of solution. For instance, a constant flow simply translates the field as a whole without making the X-point collapse, while $v_0 = -z$ represents an inflow which just concentrates the field and $v_0 = \mathrm{i}z$ gives a circular flow which also decreases the field magnitude, again without producing a current sheet. Apart from flows of the form (4.33), we are therefore left only with solutions approaching z_0^{-1} as z_0 tends to zero, or behaving like z_0^{-n}.

An example of the former would be to adopt

$$v_0 = \frac{\pi}{8L} \Big/ \sinh\left(\frac{\pi z_0}{2L}\right), \tag{4.34}$$

so that

$$v_{1x} = \left(\frac{\pi}{8L}\right) \sinh\left(\frac{\pi x}{2L}\right) \cos\left(\frac{\pi y}{2L}\right) \Big/ \left\{\sinh^2\left(\frac{\pi x}{2L}\right) + \sin^2\left(\frac{\pi y}{2L}\right)\right\},$$

$$v_{1y} = -\left(\frac{\pi}{8L}\right) \cosh\left(\frac{\pi x}{2L}\right) \sin\left(\frac{\pi y}{2L}\right) \Big/ \left\{\sinh^2\left(\frac{\pi x}{2L}\right) + \sin^2\left(\frac{\pi y}{2L}\right)\right\}.$$

This behaves like (4.31) near the origin and has $v_x = 0$ on $x = 0$ and $v_y = 0$ on $y = 0$, but at $y = \pm L$ it represents a unidirectional inflow with $v_x = 0$. However, the inversion of (4.32) is then not possible analytically in terms of elementary functions.

The initial flow

$$v_0 = \frac{1}{z_0^3} \tag{4.35}$$

represents a flow that comes in on the asymptotes $\theta = \pm\frac{1}{4}\pi$, $\theta = \pm\frac{3}{4}\pi$ and goes out along the x- and y-axes. Equation (4.32) then becomes

$$z_0^4 - z z_0^3 + t = 0,$$

with four roots, one of which is

$$z_0 = b + \sqrt{(b^2 - c)}, \tag{4.36}$$

where

$$b = \tfrac{1}{2}[\tfrac{1}{2}z + (\tfrac{1}{4}z^2 + u)^{1/2}], \quad c = \tfrac{1}{2}u + (\tfrac{1}{4}u^2 - t)^{1/2}$$

and

$$u = \{\tfrac{1}{2}t[z^2 - (z^4 - \tfrac{256}{27}t)^{1/2}]\}^{1/3} + \{\tfrac{1}{2}t[z^2 + (z^4 - \tfrac{256}{27}t)^{1/2}]\}^{1/3}.$$

The resulting field therefore has a complex flux function of $f = \frac{1}{2}z_0^2$ with $z_0(z,t)$ given by (4.36). The flow (4.35) makes a double current sheet grow from the origin with its ends at

$$z = \pm\frac{4t^{1/4}}{3^{3/4}}, \quad \text{and} \quad z = \pm\frac{4\mathrm{i}t^{1/4}}{3^{3/4}}.$$

Similarly, the flow $v_0 = z_0^{-5}$ would come in along the y-axis and go out along the x-axis, but would also be inflowing along a direction $\pm\frac{1}{6}\pi$ and outflowing along $\pm\frac{1}{3}\pi$.

PHILOSOPHICAL TRANSACTIONS OF THE ROYAL SOCIETY A MATHEMATICAL, PHYSICAL & ENGINEERING SCIENCES

(*g*) *Accelerated flows*

In the process of setting up our basic solution (2.26), we have assumed that the arbitrary function $\chi(t)$ in (2.18) is identically zero, and so the general solution to (2.18), namely

$$\frac{\partial^2 z}{\partial t^2} = \chi(t)\frac{\partial z}{\partial f}, \tag{4.37}$$

became

$$z = z_0 + v_0 t$$

and the flows were acceleration-free in the sense that $\partial^2 z/\partial t^2 = 0$. Let us therefore briefly consider some of the consequences of having accelerated flows for which $\partial^2 z/\partial t^2 \neq 0$.

First, suppose $\chi(t) = \chi_0$, a constant. Then the general solution to (4.37) having $z = z_0(f)$ and $\partial z/\partial t = v_0(f)$ at $t = 0$ is

$$z(f,t) = z_0(f) + v_0(f)t + \tfrac{1}{2}\chi_0\frac{\mathrm{d}z_0}{\mathrm{d}f}t^2 + \sum_{k=1}^{\infty}\left(\frac{\mathrm{d}^k v_0}{\mathrm{d}f^k}\frac{\chi_0^k t^{2k+1}}{(2k+1)!} + \frac{\mathrm{d}^{k+1}z_0}{\mathrm{d}f^{k+1}}\frac{\chi_0^{k+1}t^{2k+2}}{(2k+2)!}\right). \tag{4.38}$$

In particular, if we adopt our basic initial state

$$f_0 = \tfrac{1}{2}z_0^2$$

and initial flow

$$v_0 = \frac{c^2}{z_0},$$

then for sufficiently small time t or acceleration χ_0, (4.38) may be approximated by

$$z \approx z_0 + \frac{c^2 t}{z_0} + \frac{\chi_0 t^2}{2z_0}. \tag{4.39}$$

The solution for the complex potential is then $f = \frac{1}{2}z_0^2$, where

$$2z_0 = z + \sqrt{(z^2 - 4c^2t - 2\chi_0 t^2)},$$

and so the ends of the current sheet are now located at

$$z = \pm\sqrt{(4c^2t + 2\chi_0 t^2)}$$

in place of $\pm 2c\sqrt{t}$. If, therefore, the acceleration is positive ($\chi_0 > 0$), the ends of the current sheet move outwards faster. If it is negative, they move more slowly out to a distance $\sqrt{2c^2}/\sqrt{(-\chi_0)}$ at $t = -c^2/\chi_0$, and then they reverse direction and move inwards; at $t = -2c^2/\chi_0$ the sheet vanishes and thereafter it grows along the y-axis.

The particular case when $c = 0$, so $v_0(f) \equiv 0$, is of particular interest since it implies that the plasma is initially at rest, a possibility which was not allowed in our basic solutions. Then the ends of the sheet are located at $\pm\sqrt{(2\chi_0)}t$ and so move with constant velocity. The resulting magnetic field and velocity are given by

$$B_{0y} + \mathrm{i}B_{0x} = -\frac{\partial f}{\partial z} = -\frac{[z + \sqrt{(z^2 - 2\chi_0 t^2)}]^2}{4\sqrt{(z^2 - 2\chi_0 t^2)}} \tag{4.40}$$

PHILOSOPHICAL TRANSACTIONS OF THE ROYAL SOCIETY A MATHEMATICAL, PHYSICAL & ENGINEERING SCIENCES

and

$$v_{1x} + \mathrm{i}v_{1y} = \frac{\partial z}{\partial t} = \frac{2\chi_0 t}{z + \sqrt{(z^2 - 2\chi_0 t^2)}}, \tag{4.41}$$

so that the field and flow components are self-similar with a similarity variable z/t in place of $z/\sqrt{t}$. The corresponding electric field is

$$E_0 = -\operatorname{Re}\mathcal{VB} = -\frac{\chi_0 t}{2}\operatorname{Re}\left(1 + \frac{z}{\sqrt{(z^2 - 2\chi_0 t^2)}}\right),$$

which vanishes at $t = 0$, and the density is

$$\rho = \frac{\rho_0}{|\partial z/\partial z_0|^2} = \frac{\rho_0}{|1 - 2\chi_0 t^2/[z + \sqrt{(z^2 - 2\chi_0 t^2)}]^2|^2}.$$

At the current sheet, $B_{0y} = -\frac{1}{2}x$ as before. The current density is

$$J = \frac{\chi_0 t^2 - x^2}{\mu\sqrt{(2\chi_0 t^2 - x^2)}},$$

which reverses direction at $x = \pm\sqrt{\chi_0 t}$; the total current in the sheet vanishes, as expected from the current conservation. The paths of plasma elements are given, by eliminating t between the real and imaginary parts of (4.39), simply as the straight lines

$$\frac{x}{x_0} + \frac{y}{y_0} = 2.$$

Although moving in straight lines, the plasma elements are accelerating since their speeds are increasing linearly with time, as can be seen by rewriting the velocity components (4.41) as

$$v_x + \mathrm{i}v_y = \frac{\chi_0 t}{z_0}.$$

When $\chi(t)$ is a given function of t, one needs, in general, to resort to numerical techniques to solve (4.37) with the appropriate initial conditions. However, at small time, if $\chi \approx \chi_0 t^n$, the corresponding form to (4.39) is

$$z \approx z_0 + \frac{c^2 t}{z_0} + \frac{\chi_0 t^{n+2}}{(n+1)(n+2)z_0},$$

and so, in the subsequent solutions with $c^2 = 0$, one simply replaces $\frac{1}{2}t^2$ by $t^{n+2}/[(n+1)(n+2)]$.

Also, in general, if χ can be expanded in powers of t as

$$\chi(t) = \sum_{m=0}^{\infty} \chi_m t^m, \tag{4.42}$$

say, and we adopt the standard initial conditions, namely

$$z(0, f) = z_0(f), \quad \frac{\partial z}{\partial t}(0, f) = v_0(f), \tag{4.43}$$

then the solution of (4.37) may be obtained as a power series in t:

$$z(t, f) = \sum_{k=0}^{\infty} t^k a_k(f).$$

After substituting this expansion into equation (4.37), we obtain a recurrence relation for the required coefficients as

$$a_k(f) = \sum_{n=0}^{k-2} \chi_{k-2-n} a'_n(f)/[(k-1)k], \quad k = 2, 3, \ldots, \tag{4.44}$$

where

$$a_0(f) = z_0(f) \quad \text{and} \quad a_1(f) = v_0(f). \tag{4.45}$$

Relationships (4.44) and (4.45) therefore determine the general solution to the initial-value problem.

We may apply these relationships for a particular example, namely the function

$$\chi(t) \equiv \chi_1 t, \tag{4.46}$$

where $\chi_1 =$ constant. In this case, (4.44) gives

$$a_2(f) \equiv 0,$$

and

$$a_k(f) = \frac{\chi_1 a'_{k-3}(f)}{(k-1)k}, k = 3, 4, \ldots.$$

Applying (4.47) repeatedly, we then obtain all the required coefficients explicitly as

$$a_{3m+2}(f) = 0,$$

$$a_{3m}(f) = \frac{\chi_1^m z_0^{(m)}(f)}{3^m m! \Pi_{l=1}^m (3l-1)},$$

$$a_{3m+1}(f) = \frac{\chi_1^m v_0^{(m)}(f)}{3^m m! \Pi_{l=1}^m (3l+1)},$$

where $m = 1, 2, \ldots$. In the same way, it is possible to find the general solution for any polynomial function $\chi(t)$.

5. Solutions with unfrozen potential

(*a*) *General method of solution*

We have been able to derive a wide class of analytical solutions to the basic equations (2.7)–(2.9), or equivalently (2.11)–(2.13), namely

$$\boldsymbol{j}_0 = 0, \tag{5.1a}$$

$$\frac{\partial \boldsymbol{B}_0}{\partial t} = \nabla \times (\boldsymbol{v}_1 \times \boldsymbol{B}_0), \tag{5.1b}$$

$$\frac{\mathrm{d}\boldsymbol{v}_1}{\mathrm{d}t} \cdot \boldsymbol{B}_0 = 0, \tag{5.1c}$$

or

$$\nabla^2 A = 0, \tag{5.2a}$$

$$\frac{\mathrm{d}A}{\mathrm{d}t} = 0, \tag{5.2b}$$

$$\frac{\mathrm{d}\boldsymbol{v}_1}{\mathrm{d}t} \times \nabla A = 0, \tag{5.2c}$$

by making the additional assumption that the magnetic potential (Φ) remains frozen to the plasma. When this assumption is relaxed, it is much more difficult to make analytical progress and, in general, a numerical technique is required.

In principle, one may consider any topologically accessible set of potential solutions to (5.1a) or (5.2a) for the magnetic field and then the flow speed normal to the magnetic field $v_{1\perp}$ is determined explicitly by (5.1b) or (5.2b). The difficult step is finally to solve the nonlinear equation (5.1c) or (5.2c) for the flow speed parallel to the magnetic field $v_{1\parallel}$.

Now the plasma velocity ($\boldsymbol{v_1}$) may be written as

$$\boldsymbol{v_1} = v_\perp \hat{\boldsymbol{n}} + v_\parallel \hat{\boldsymbol{s}}, \tag{5.3}$$

where $\hat{\boldsymbol{n}}$ and $\hat{\boldsymbol{s}}$ are unit vectors normal and parallel to the magnetic field, respectively. In terms of the assumed known magnetic flux function A and potential Φ, these unit vectors may be written

$$\hat{\boldsymbol{n}} = \frac{\nabla A}{B_0}, \quad \hat{\boldsymbol{s}} = \frac{\nabla \Phi}{B_0}, \tag{5.4}$$

where $A(\boldsymbol{r}, t)$ and $\Phi(\boldsymbol{r}, t)$ satisfy the Cauchy–Riemann equations

$$\frac{\partial A}{\partial x} = \frac{\partial \Phi}{\partial y}, \quad \frac{\partial A}{\partial y} = -\frac{\partial \Phi}{\partial x}. \tag{5.5}$$

Equation (5.2b) may be written

$$\frac{\partial A}{\partial t} + \boldsymbol{v_1} \cdot \nabla A \equiv \frac{\partial A}{\partial t} + v_{1\perp} B_0 = 0,$$

and so the perpendicular velocity component is given simply by

$$v_{1\perp} = \frac{-\partial A/\partial t}{B_0} \tag{5.6}$$

once $A(\boldsymbol{r}, t)$ and $\boldsymbol{B}(\boldsymbol{r}, t)$ are imposed.

Next we may write $v_{1\parallel}$ in terms of an unknown function σ as

$$v_{1\parallel} = \frac{\sigma}{B_0}, \tag{5.7}$$

so that (5.3) becomes

$$\boldsymbol{v_1} = -\frac{\partial A/\partial t}{B_0}\hat{\boldsymbol{n}} + \frac{\sigma}{B_0}\hat{\boldsymbol{s}}. \tag{5.8}$$

Then, taking the scalar product with $\boldsymbol{B}$ and noting that $\boldsymbol{B} = B\hat{\boldsymbol{s}}$, we find

$$\sigma = \boldsymbol{v_1} \cdot \boldsymbol{B}_0, \tag{5.9}$$

so that σ represents the local cross helicity (whose global average is a rugged invariant in MHD turbulence theory). Operating on this with $\mathrm{d}/\mathrm{d}t$ and using (5.1c), we obtain

$$\frac{\mathrm{d}\sigma}{\mathrm{d}t} = \boldsymbol{v_1} \cdot \frac{\mathrm{d}\boldsymbol{B}_0}{\mathrm{d}t}, \tag{5.10}$$

PHILOSOPHICAL TRANSACTIONS OF THE ROYAL SOCIETY A MATHEMATICAL, PHYSICAL & ENGINEERING SCIENCES

which determines σ and, hence from (5.7), $v_{\|}$. Equation (5.10) is not as simple as it first appears, since $\boldsymbol{v}$, given by (5.8), involves σ and, in terms of Eulerian coordinates, is a partial differential equation.

However, it may be solved by the method of characteristics (Titov 1995): in terms of Lagrangian coordinates, σ and the coordinates (x, y) of a plasma element are given by three ordinary differential equations of the form

$$\frac{\mathrm{d}\sigma}{\mathrm{d}t} = g(x, y, t, \sigma), \quad \frac{\mathrm{d}x}{\mathrm{d}t} = v_x(x, y, t, \sigma), \quad \frac{\mathrm{d}y}{\mathrm{d}t} = v_y(x, y, t, \sigma), \tag{5.11}$$

where, from (5.4), (5.5), (5.8),

$$v_{1x} = \frac{\partial A/\partial t}{B_0^2} B_{0y} + \frac{\sigma}{B_0^2} B_{0x}, \quad v_{1y} = -\frac{\partial A/\partial t}{B_0^2} B_{0x} + \frac{\sigma}{B_0^2} B_{0y}, \tag{5.12}$$

and (5.10) gives

$$g = v_{1x}\left(\frac{\partial B_{0x}}{\partial t} + v_{1x}\frac{\partial B_{0x}}{\partial x} + v_{1y}\frac{\partial B_{0x}}{\partial y}\right) + v_{1y}\left(\frac{\partial B_{0y}}{\partial t} + v_{1x}\frac{\partial B_{0y}}{\partial x} + v_{1y}\frac{\partial B_{0y}}{\partial y}\right), \tag{5.13}$$

where

$$\frac{\partial B_{0x}}{\partial x} = -\frac{\partial B_{0y}}{\partial y}, \quad \text{and} \quad \frac{\partial B_{0y}}{\partial x} = \frac{\partial B_{0x}}{\partial y},$$

so that, in cases where one of these partial derivatives is undefined in (5.13), it may be replaced by another.

In terms of the complex magnetic field $\mathcal{B}(z, t) = B_{0y} + \mathrm{i}B_{0x}$ and velocity function $\mathcal{V}(z, t) = v_{1x} + \mathrm{i}v_{1y}$, equations (5.11) may be rewritten more compactly as

$$\frac{\mathrm{d}\sigma}{\mathrm{d}t} = \mathrm{Im}\left\{\mathcal{V}\left(\frac{\partial \mathcal{B}}{\partial t} + \mathcal{V}\frac{\partial \mathcal{B}}{\partial z}\right)\right\}, \tag{5.14a}$$

$$\frac{\mathrm{d}x}{\mathrm{d}t} = \mathrm{Re}\,\mathcal{V}, \tag{5.14b}$$

$$\frac{\mathrm{d}y}{\mathrm{d}t} = \mathrm{Im}\,\mathcal{V}, \tag{5.14c}$$

where

$$\mathcal{V} = \frac{\partial A/\partial t + \mathrm{i}\sigma}{\mathcal{B}}. \tag{5.15}$$

Thus, for any sequence $\boldsymbol{B}_0(x, y, t)$ or $\mathcal{B}(z, t)$ of accessible magnetic configurations under the strong magnetic field approximation, the flow velocity components are given by (5.6) and (5.7), with σ determined by (5.11) or (5.14). For a steady-state situation, $\partial \mathcal{B}/\partial t = 0$ in (5.14*a*), and (5.15) becomes

$$\mathcal{V} = \frac{-E_0 + \mathrm{i}\sigma}{\mathcal{B}},$$

where the electric field E_0 is a constant.

Once the velocity components have been found, the density is determined by the continuity equation

$$\frac{\partial \rho}{\partial t} + (\boldsymbol{v_1} \cdot \nabla)\rho = -\rho \nabla \cdot \boldsymbol{v_1}. \tag{5.16a}$$

Calculating the density in terms of the Jacobian of the mapping from initial positions ($\boldsymbol{r}_0$) to final positions ($\boldsymbol{r}$), as in equation (2.30), is not easily possible since the mapping is determined numerically by (5.14). Furthermore, at first sight, the method of characteristics seems to be not possible since $\nabla \cdot \boldsymbol{v}_1$ on the right-hand side of (5.16) involves knowing $\nabla\sigma$. However, $\nabla\sigma$ is in turn given from (5.10) by

$$\frac{\partial \nabla\sigma}{\partial t} + (\boldsymbol{v}_1 \cdot \nabla)\nabla\sigma = \nabla g - (\nabla \boldsymbol{v}_1) \cdot \nabla\sigma. \tag{5.16b}$$

Thus, ρ and $\nabla\sigma$ may be obtained from (5.16a) and (5.16b) by the method of characteristics. In complex form, we obtain the following ordinary differential equations:

$$\frac{\mathrm{d}\rho}{\mathrm{d}t} = \rho \,\mathrm{Re}\left[\frac{1}{\mathcal{B}}\left(\frac{\partial \mathcal{B}}{\partial t} + 2\mathcal{V}\frac{\partial \mathcal{B}}{\partial z} - \mathcal{S}\right)\right],$$

$$\frac{\mathrm{d}\mathcal{S}}{\mathrm{d}t} = \mathcal{V}\left(\frac{\partial^2 \mathcal{B}}{\partial t \partial z} - \frac{1}{\mathcal{B}}\frac{\partial \mathcal{B}}{\partial t}\frac{\partial \mathcal{B}}{\partial z}\right) - \mathrm{i}\frac{\partial \mathcal{B}}{\partial t}\,\mathrm{Im}\left[\frac{1}{\mathcal{B}}\left(\frac{\partial \mathcal{B}}{\partial t} + 2\mathcal{V}\frac{\partial \mathcal{B}}{\partial z} - \mathcal{S}\right)\right]$$
$$+\mathcal{V}^2\left[\frac{\partial^2 \mathcal{B}}{\partial z^2} - \frac{2}{\mathcal{B}}\left(\frac{\partial \mathcal{B}}{\partial z}\right)^2\right] + \mathcal{S}\frac{\mathcal{V}}{\mathcal{B}}\frac{\partial \mathcal{B}}{\partial z} + \mathcal{S}\,\mathrm{Re}\left[\frac{1}{\mathcal{B}}\left(\frac{\partial \mathcal{B}}{\partial t} + 2\mathcal{V}\frac{\partial \mathcal{B}}{\partial z} - \mathcal{S}\right)\right],$$

where $\mathcal{S}$ is a complex variable whose real and imaginary parts are the y- and x-components of $\nabla\sigma$, respectively. These equations may be solved together with (5.14) and their solutions define the positions of the moving particles at time t and the corresponding values of σ, ρ, and $\nabla\sigma$ for these particles. For flows in stationary magnetic fields, the above equations are significantly simplified to

$$\frac{\mathrm{d}\rho}{\mathrm{d}t} = \rho \,\mathrm{Re}\left[\frac{1}{\mathcal{B}}\left(2\mathcal{V}\frac{\mathrm{d}\mathcal{B}}{\mathrm{d}z} - \mathcal{S}\right)\right],$$

$$\frac{\mathrm{d}\mathcal{S}}{\mathrm{d}t} = \mathcal{V}^2\left[\frac{\mathrm{d}^2 \mathcal{B}}{\mathrm{d}z^2} - \frac{2}{\mathcal{B}}\left(\frac{\mathrm{d}\mathcal{B}}{\mathrm{d}z}\right)^2\right] + \mathcal{S}\frac{\mathcal{V}}{\mathcal{B}}\frac{\mathrm{d}\mathcal{B}}{\mathrm{d}z} + \mathcal{S}\,\mathrm{Re}\left[\frac{1}{\mathcal{B}}\left(2\mathcal{V}\frac{\mathrm{d}\mathcal{B}}{\mathrm{d}z} - \mathcal{S}\right)\right].$$

Thus, determining all the physical values in hypersonic MHD flows has been reduced to solving ordinary differential equations.

(*b*) *Formation of a current sheet with Y-point ends*

As an example, we now apply the above general method to the particular case of a growing current sheet with Y-type null points at its ends. The assumed complex magnetic field is

$$\mathcal{B}(z,t) = (z^2 - L^2)^{1/2}, \tag{5.17}$$

where $L(t)$ is a growing function of t and the current sheet extends between $x = -L$ and $x = +L$ along the x-axis. Equations (5.14) then reduce to

$$\frac{\mathrm{d}\sigma}{\mathrm{d}t} = \mathrm{Im}\left[\frac{(z\mathcal{V} - L\dot{L})\mathcal{V}}{(z^2 - L^2)^{1/2}}\right], \tag{5.18}$$

$$\frac{\mathrm{d}x}{\mathrm{d}t} = \mathrm{Re}\,\mathcal{V}, \quad \frac{\mathrm{d}y}{\mathrm{d}t} = \mathrm{Im}\,\mathcal{V},$$

where

$$\mathcal{V} = \frac{\mathrm{Re}(L\dot{L}\cosh^{-1} z/L) + \mathrm{i}\sigma + \dot{F}}{(z^2 - L^2)^{1/2}}.$$

Here $F(t)$ is an arbitrary function of time which arises from the integration of $-\mathcal{B}$ with respect to z to give $f(z,t) = A + \mathrm{i}\Phi$. Thus, from (5.17) we find

$$f(z) = -\tfrac{1}{2}z(z^2 - L^2)^{1/2} + \tfrac{1}{2}L^2 \cosh^{-1}(z/L) + F(t) \tag{5.19}$$

and so $F(t)$ represents the value of the flux function A at the ends $z = \pm L$ of the sheet. If $F(t) \equiv$ const., then there is no reconnection, whereas, if, for example, $F(t) = -E_0 t$ with E_0 constant, there is a constant rate of reconnection as flux passes through the current sheet at a constant rate.

For some practical purposes, the real form (5.11) of the equations is more useful, even though (5.18) is more elegant. From (5.17) it can be shown that the field components (B_{0x}, B_{0y}) are given by

$$B_{0x} = s, \quad B_{0y} = r, \tag{5.20}$$

where

$$\begin{aligned} 2s^2 &= \sqrt{(X^2 + Y^2)} - X \\ 2r^2 &= \sqrt{(X^2 + Y^2)} + X \\ X &= x^2 - y^2 - L^2 \\ Y &= 2xy. \end{aligned} \tag{5.21}$$

The corresponding flux function is

$$A = \tfrac{1}{2}(-xr + ys + L^2 \log\{[(x+r)^2 + (y+s)^2]^{1/2}/L\}) + F(t) \tag{5.22}$$

and its time derivative is

$$\frac{\partial A}{\partial t} = L\dot{L} \log\{[(x+r)^2 + (y+s)^2]^{1/2}/L\} + \dot{F}. \tag{5.23}$$

The remaining expressions that are required for solving (5.11) are

$$\frac{\partial B_{0x}}{\partial t} = -\frac{[X(X^2+Y^2)^{-1/2} - 1]L\dot{L}}{2s}, \quad \frac{\partial B_{0y}}{\partial t} = -\frac{[X(X^2+Y^2)^{-1/2} + 1]L\dot{L}}{2r},$$

$$\frac{\partial B_{0y}}{\partial y} = -\frac{1}{2r}\left(\frac{xY - yX}{\sqrt{X^2+Y^2}} - y\right), \quad \frac{\partial B_{0y}}{\partial x} = \frac{1}{2r}\left(\frac{xX + yY}{\sqrt{X^2+Y^2}} + x\right),$$

$$\frac{\partial B_{0x}}{\partial x} = \frac{1}{2s}\left(\frac{xX + yY}{\sqrt{X^2+Y^2}} - x\right), \quad \frac{\partial B_{0x}}{\partial y} = \frac{1}{2s}\left(\frac{xY - yX}{\sqrt{X^2+Y^2}} - y\right).$$

We consider two particular cases where σ is initially assumed equal to zero. In the first, the length of the current sheet is assumed to grow linearly in time $(L = t)$, while $F(t) \equiv 0$ so that there is no reconnection. The resulting paths and velocity components of plasma elements in the first quadrant are shown in figure 11, where the initial field lines are shown dashed. Elements which start above the separatrix approach the x-axis and initially follow roughly straight-line paths, but when they are close to the x-axis they curve rapidly as the flow speed $v_{1\parallel}$ along the field lines becomes much greater than the speed $v_{1\perp}$ normal to the field lines, and the velocity becomes tangential to the x-axis. For the first few time elements, the field line rotates slightly in an anticlockwise direction and a negative $v_{1\parallel}$ is produced. Thereafter, as a substantial current sheet forms, the field line rotates in a clockwise direction: this produces a coriolis force $(-m\boldsymbol{\omega}_1 \times \boldsymbol{v}_1)$ acting to the left which makes the particle path bend to the left and which is balanced by a

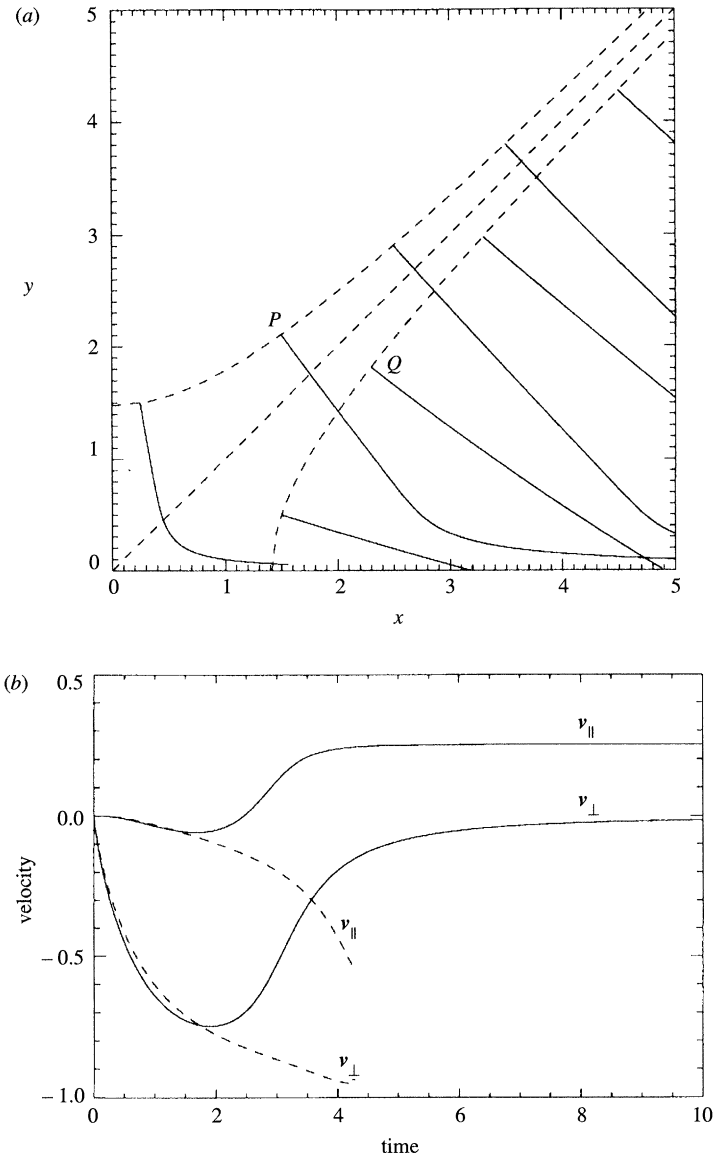

Figure 11. (a) Paths of plasma elements when $L = t$ and $F(t) = 0$. (b) Velocity components of plasma elements initially at P (solid) and Q (dotted).

centrifugal force acting to the right. Elements which start ahead of the separatrix, on the other hand, continue in paths which are only slightly curved. Eventually, they reach the x-axis ahead of the current sheet and with a non-zero y-component of velocity. At this point the analysis fails and one would expect a weak shock wave to form.

For the second case, we have held the sheet length constant ($L = 1$) and set $F(t) = -t$, so that we have steady reconnection. The paths of plasma elements and their velocity components are shown in figure 12. The magnetic field lines are shown dashed in figure 12a. Elements P and Q are both on field lines which are locally rotating in an anticlockwise direction and so the coriolis force acts to the

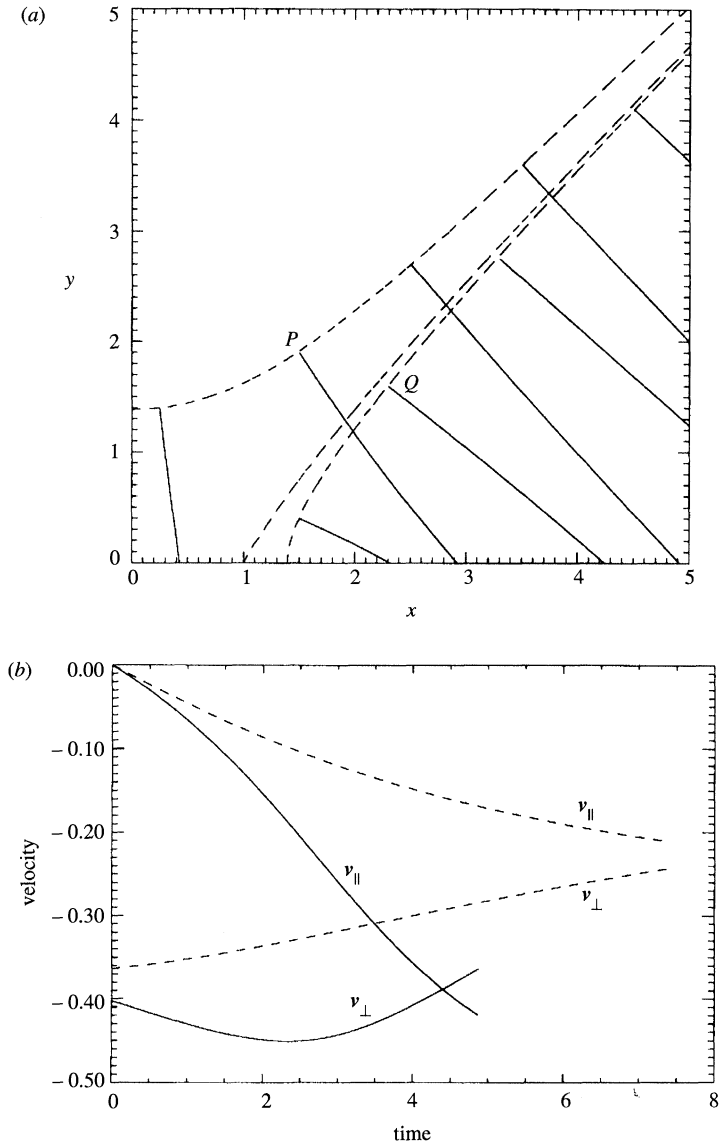

Figure 12. (*a*) Paths of plasma elements when $L = 1$ and $F(t) = -t$. (*b*) Velocity components of plasma elements initially at P (solid) and Q (dotted).

right as the plasma element moves and generates a negative $v_\parallel$. They eventually reach the x-axis with a non-zero y-component of velocity and would be expected to create a weak shock wave that is beyond the scope of the present analysis.

6. Conclusion

Until now, only two basic solutions for the formation of singularities in a magnetic field near an X-point have been put forward, namely the Green solution,

$$B_{0y} + \mathrm{i}B_{0x} = (z^2 + L^2)^{1/2},$$

and the Syrovatsky–Somov solution,

$$B_{0y} + \mathrm{i}B_{0x} = \frac{z^2 + a^2}{(z^2 + L^2)^{1/2}}.$$

In the present paper, we have discovered a large family of analytical solutions which are, like the above solutions, potential outside the singularity, but which are also self-consistent solutions of the MHD equations in the strong magnetic field approximation of time-dependent slow flow in an ideal low-beta plasma.

Analytical progress is made by assuming that the magnetic potential is frozen to the plasma and considering, in particular, acceleration-free flows from the initial field $(B_{0x}, B_{0y}) = (-y, -x)$. The resulting solution is expressed in compact complex form as

$$B_{0y} + \mathrm{i}B_{0x} = -\frac{(z + \sqrt{(z^2 - t)})^2}{4\sqrt{(z^2 - t)}}.$$

A current sheet stretches between $-\sqrt{t}$ and $+\sqrt{t}$ on the x-axis, and as it grows it swallows half of the magnetic flux, while the remainder piles up ahead of the sheet and creates regions of reversed current near the ends.

A current conservation theorem is proved, which states that the total current in the sheet vanishes if the flux function and magnetic potential are conserved. In addition, the basic solution is generalized in many ways to consider different initial magnetic configurations, which have been proposed previously, and flows which are accelerated. Also, a general numerical method for finding solutions with unfrozen potential is developed and is applied to the Green solution with Y-points at the ends of the current sheet.

The general topic of MHD behaviour near an X-point is enormous and has been studied under a wide range of different assumptions. The present study of time-dependent nonlinear ideal collapse aims to increase our understanding by complementing the traditional theories of magnetic reconnection in a different region of parameter space. In future, it would be invaluable to include pressure-gradient, resistive and weak shock effects. However, the general methods developed here would also be of use for non-X-point studies of the time-dependent evolution of magnetic configurations.

E.R.P. is delighted to acknowledge stimulating conversations with Dionysis Linardatos, Keith Moffatt, Mike Proctor, Andrew Soward and Nigel Weiss at the Isaac Newton Institute in Cambridge, where the bulk of this work was undertaken. He is also grateful to the UK Science and Engineering Research Council for financial support.

References

Aly, J. J. & Amari, T. 1989 *Astron. Astrophys.* **221**, 287.

Bajer, K. 1990 Ph.D. thesis, Cambridge University.

Biskamp, D. 1986 *Physics Fluids* **29**, 1520.

Craig, I. J. D. & McClymont, A. N. 1991 *Astrophys. J.* **371**, L41–L44.

Dungey, J. W. 1953 *Phil. Mag.* **44**, 725–738.

Forbes, T. G. 1982 *J. Plasma Phys.* **27**, 491–505.

Forbes, T. G. & Priest, E. R. 1987 *Rev. Geophys.* **25**, 1583–1607.

Forbes, T. G. & Speiser, T. W. 1979 *J. Plasma Phys.* **21**, 107.

Green, R. M. 1965 *IAU Symp.* **2**, 398–404.

PHILOSOPHICAL TRANSACTIONS OF THE ROYAL SOCIETY A MATHEMATICAL, PHYSICAL & ENGINEERING SCIENCES

Imshennik, V. S. & Syrovatsky, S. I. 1967 *Soviet. Phys. JETP* **25**, 656–664.

Lee, L. C. & Fu, Z. F. 1986 *J. Geophys. Res.* **91**, 6807.

Linardatos, D. 1993 *J. Fluid Mech.* **246**, 569–591.

Low, B. C. & Hu, Y. Q. 1983 *Solar Phys.* **84**, 83–98.

Malherbe, J. M. & Priest, E. R. 1983 *Astron. Astrophys.* **123**, 80–88.

Moffatt, H. K. 1985 *J. Fluid Mech.* **159**, 359–378.

Moffatt, H. K. 1990 *Phil. Trans. R. Soc. Lond.* A 333, 321–342.

Parker, E. N. 1972 *Astrophys. J.* **174**, 499–510.

Priest, E. R. (ed.) 1981 *Solar flare magnetohydrodynamics.* Gordon & Breach.

Priest, E. R. 1985 *Rep. Prog. Phys* **48**, 955–1090.

Priest, E. R. 1993 In *Physics of solar and stellar coronae* (ed. J. K. Linsky & S. Serio), pp. 515–532. Dordrecht: Kluwer.

Priest, E. R., Hood, A. W. & Anzer, U. 1989 *Astrophys. J.* **344**, 1010–1025.

Priest, E. R. & Lee, L. C. 1990 *J. Plasma Phys.* **44**, 337–360.

Priest, E. R., Parnell, C. E. & Martin, S. F. 1994 *Astrophys. J.* **427**, 459–474.

Priest, E. R. & Raadu, M. A. 1975 *Solar Phys.* **43**, 177–188.

Sakurai, T. & Uchida, Y. 1977 *Solar Phys.* **52**, 397.

Somov, B. V. 1992 *Physical processes in solar flares.* Dordrecht: Kluwer.

Somov, B. V. & Syrovatsky, S. I. 1976 *Proc. Lebedev Phys. Inst.* **74**, 13–72.

Strachan, N. R. & Priest, E. R. 1994, *Geophys. Astrophys. Fluid Dynamics* **74**, 245–274.

Svestka, Z, Jackson, B. V. & Machado, M. E. 1992 *Eruptive solar flares.* Springer.

Syrovatsky, S. I. 1966 *Soviet Astron.* **10**, 270–280.

Syrovatsky, S. I. 1969 *Solar flares and space research* (ed. C. de Jager & Z. Svestka), pp. 346–355. Amsterdam: North-Holland.

Syrovatsky, S. I. 1971 *Soviet Phys. JETP* **33**, 933–940.

Titov, V. S. 1992 *Solar Phys.* **139**, 401–404.

Titov, V. S. 1995 *Geometry in partial differential equations.* Singapore: World Scientific. (In the press.)

Titov, V. S. & Priest, E. R. 1993, *Geophys. Astrophys. Fluid Dynamics* **72**, 249–276.

Tur, T. J. 1977 Ph.D. thesis, St Andrews University.

Tur, T. J. & Priest, E. R. 1976 *Solar Phys.* **48**, 89–100.

Ulmschneider, P., Priest, E. R. & Rosner, R. 1991 *Mechanisms of chromospheric and coronal heating.* Springer.

Received 5 July 1993; accepted 26 July 1994

PHILOSOPHICAL TRANSACTIONS OF THE ROYAL SOCIETY A MATHEMATICAL, PHYSICAL & ENGINEERING SCIENCES